

Nanoscale

Accepted Manuscript



This is an *Accepted Manuscript*, which has been through the Royal Society of Chemistry peer review process and has been accepted for publication.

Accepted Manuscripts are published online shortly after acceptance, before technical editing, formatting and proof reading. Using this free service, authors can make their results available to the community, in citable form, before we publish the edited article. We will replace this *Accepted Manuscript* with the edited and formatted *Advance Article* as soon as it is available.

You can find more information about *Accepted Manuscripts* in the [Information for Authors](#).

Please note that technical editing may introduce minor changes to the text and/or graphics, which may alter content. The journal's standard [Terms & Conditions](#) and the [Ethical guidelines](#) still apply. In no event shall the Royal Society of Chemistry be held responsible for any errors or omissions in this *Accepted Manuscript* or any consequences arising from the use of any information it contains.

Carbon-atom wires: 1-D systems with tunable properties

C.S. Casari,^{a,*} M. Tommasini,^b R.R. Tykwinski^c and A. Milani^b

Received 00th January 20xx,
Accepted 00th January 20xx

DOI: 10.1039/x0xx00000x

www.rsc.org/

This review provides a discussion of the current state of research on linear carbon structures and related materials based on sp -hybridization of carbon atoms (polyynes and cumulenes). We show that such systems have widely tunable properties and thus represent an intriguing and mostly unexplored field for both fundamental and applied science. We discuss the rich interplay between structural, vibrational, and electronic properties focusing on recent advances and the future perspectives of carbon-atom wires and novel hybrid sp - sp^2 -carbon architectures.

1 Introduction

Carbon is a chemically versatile element that can adopt different hybridization states to produce a wide variety of allotropic forms, molecules, and nanostructures. sp -, sp^2 -, and sp^3 -hybridized atomic orbitals give rise to linear, planar and three-dimensional organization in carbon-based molecules, (e.g., respectively alkynes, alkenes, and alkanes) as well as in condensed matter (isotropic and anisotropic structure of diamond and graphite, respectively). A crystalline solid made of sp -carbon is absent as a third allotropic form of carbon, whose existence is questionable or even considered impossible for stability reasons. Low-dimensional carbon structures comprise quasi-zero- and quasi-one-dimensional (quasi-0-D and quasi-1-D) 1-D systems such as fullerenes, carbon clusters, nanodiamond, and nanotubes, as well as graphene as a two-dimensional (2-D) system. In the last 30 years carbon nanostructures have indeed played a leading role in nanoscience and nanotechnology.^{1,2} Fullerenes, nanotubes, and graphene demonstrate that carbon can form a wide variety of structures whose properties are strongly related to structural issues such as dimensionality, hybridization, chirality and topology. Such structures are based on sp^3 -, sp^2 -, or mixed sp^2 - sp^3 -carbon hybridization as shown in the ternary diagram of Fig. 1. Following this classification, the sp -vertex is occupied by linear nanostructures and molecules in the form of carbon-atom wires (CAWs). Other possible novel structures that have been predicted can be placed along the lines connecting sp -

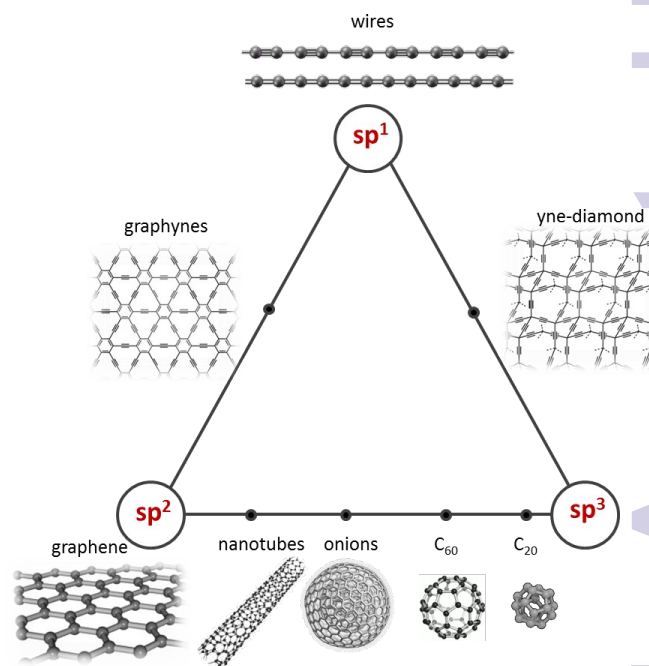


Figure 1. Ternary diagram for carbon nanostructures according to their hybridization state. Adapted with permission from C.S. Casari Istituto Lombardo (Rend. Scienze) 2012, 146, 17-35 [eISSN 2384-986X].

with sp^2 - and sp^3 -carbon, namely hybrid systems of sp - sp^2 carbon (e.g., graphyne and graphdiyne) and sp - sp^3 carbon (forms of 'superdiamond' such as yne-diamond).¹ Importantly, sp - and sp^2 -hybridized carbon systems can sustain π -conjugation, which is the basis of the metallic properties of graphene and carbon nanotubes. Graphene is a zero-gap material with outstanding electronic and optical properties for advanced technological applications (e.g., extremely high electron mobility, ambipolar conductivity related with Dirac's cones, and optical transparency).³⁻⁵

^a Department of Energy, Politecnico di Milano, via Ponzio 34/3, 20133 Milano Italy.

^b Department of Chemistry, Materials and Chemical Engineering 'G. Natta' Politecnico di Milano Piazza Leonardo da Vinci 32, 20133 Milano, Italy.

^c Department of Chemistry and Pharmacy & Interdisciplinary Center for Molecular Materials (ICMM), Friedrich-Alexander-Universität Erlangen-Nürnberg (FAU), Henkestrasse 42, 91054 Erlangen Germany.

* Corresponding author: Carlo S. Casari

e-mail: carlo.casari@polimi.it

phone: +39 023 2399 6331

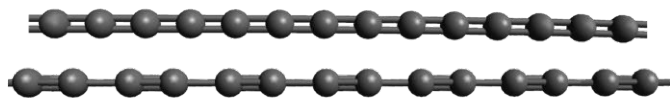


Figure 2. The two possible structures of the ideal infinite carbon-atom wire (carbyne): equalized structure with double bonds (cumulene, top) and alternate single-triple bonds (polyynes, bottom).

Opening a band gap in graphene requires additional strategies such as the exploitation of confinement effects, as it happens in graphene nanoribbons. In carbon nanotubes the electronic properties, including the semiconducting behaviour, are dominated by topological issues defined by the choice of the chiral vector and can thus be tuned to some extent.⁶ However the control of the chirality is still an open issue, which makes it difficult to tune the electronic properties of these systems.

As graphene is today considered the ultimate 2-dimensional (2-D) system (1-atom-thick) showing peculiar electronic properties, CAWs represent a true 1-D system (1-atom-diameter) that might display either semiconducting or metallic properties due to π -conjugation effects.^{7,8} In fact, in an extended linear sp-carbon system forming a CAW, the semiconductive/metallic behaviour results from the trade-off between Peierls distortion (which favours semiconductivity) and endgroup effects, which can stabilize metallic structures. Hence, sp-hybridized CAWs are intriguing systems with structure-, length-, and endgroup-dependent properties. The model CAW can show two distinct structures: $=C=C=C=C=$ or $-C\equiv C-C\equiv C-$ (see Fig. 2). In real systems, finite length effects and endgroups play a fundamental role and drive the system to a specific degree of bond length alternation: the terminal groups affect the overall wire configuration, with an increasingly larger effect in shorter wires.⁸ Control of the electronic properties (gap, conducting character) by tuning of the wire structure may thus open new perspectives for the realization of nanoscale cables and devices, as shown by theoretical predictions but not yet fully assessed by experiments.^{9,11}

Since the first understanding that diamond and graphite were made of the same “substance” (experimentally demonstrated by S. Tennant in 1796)¹² scientists have been looking for novel carbon allotropes, including linear forms of sp-hybridized carbon. The claims of the discovery of a new allotrope based on sp-hybridized carbon, named carbyne, (the mineral form found in a meteor crater in Germany was called Chaoite) date back to the 1960s,¹³⁻¹⁶ but were never confirmed even after intense debates following some criticisms raised in the 1980s.¹⁷⁻¹⁹ In the same years astrophysics studies focused on the possible presence of linear carbon in the interstellar medium, and such studies led to the discovery of fullerenes by Kroto, Smalley and Curl.²⁰ Recently, new achievements and the ground-breaking results on graphene have again driven attention to CAWs and sp-sp²-hybrids (e.g., graphyne) as novel 1-D and 2-D systems. Hence, the general skepticism about the existence of a third solid allotrope of carbon has been replaced

by the interest in 1-D and 2-D nanoscale sp-carbon structures.^{1,21} Nowadays the occurrence of sp-hybridized carbon has been suggested in many carbon-based materials and structures, in carbon-metal moieties, embedded in matrices, after laser irradiation of polymers, in free carbon clusters, in pure sp-sp² systems, in liquids, inside carbon nanotubes (CNTs) and connecting graphene sheets.²²⁻³⁵ In addition, synthetic strategies allow us to produce long and stable sp-carbon wires with controlled length and termination.³⁶ Theoretical investigations have predicted a number of interesting vibrational, electronic, and transport properties that can be tuned by controlling the wire length and endgroups. This includes carbon wires connecting metal leads, graphene, and nanotubes as device prototypes.³⁷⁻⁴⁷

Here we review the present state of research on carbon-atom wires based on both experimental and theoretical results, with particular focus on the structure-dependent properties. The review is organized as follows. We start by discussing the structure of the ideal model system (i.e., infinite wire as a 1-D crystal), the related π -conjugation effects and the change of electronic properties as a result of the wire length and termination. Then we will review synthesis techniques towards CAWs and strategies to improve stability. We will discuss the present understanding of the structure of CAWs that mainly results from Raman and surface enhanced Raman scattering (SERS) characterization of selected CAW systems. Electronic and transport properties are then discussed within the perspectives of the use of CAWs in advanced nanotechnology applications.

2 Structural, vibrational, and electronic properties of carbon-atom wires

To discuss the structure of CAWs it is better first to clarify the existing nomenclature of sp-carbon since it is rather diversified and not fully settled. In the past, the name *carbyne* was used to indicate the solid form of sp-carbon while *Chaoite* or *white carbon* has been used for minerals or solid samples found or synthesized in laboratory.¹³ More recently, the name *carbyne* has been adopted to indicate the infinite sp-carbon wire as a model system. Similarly, *carbynoid structures* has been used to indicate finite systems or moieties comprising sp-carbon in amorphous systems. Different names have been adopted to name the isolated systems, e.g., *linear carbon chains*, *carbon monatomic chains* or *carbon atomic chains*. Here, we will refer to all these systems as carbon-atom wires – CAWs. When needed, the distinction between ideal (infinite) and real (finite) CAWs will be stated.

2.1 The ideal infinite wire: interplay between electronic and vibrational properties

Despite the apparent simplicity of a system composed by sp-hybridized carbon atoms arranged in a linear (or almost linear) geometry, the physico-chemical properties of CAWs are

from trivial, as discussed in the following section. As a first approximation, the physical properties of CAWS can be interpreted on the basis of the model of an infinite chain of carbon atoms (carbyne). This ideal model allows investigation of CAWs following a convenient solid-state physics approach, similarly to other polymeric molecular materials.⁴⁸⁻⁵³ On these grounds, even if some endgroup effects will necessarily go beyond the infinite chain model, we will show that the properties of finite length sp-carbon wires can be still discussed with reference to this simple model.^{54,55} When needed this somehow restrictive approximation can be relaxed.

Contrary to "classical" σ -bonded polymers (*e.g.*, polyethylene), due to π -conjugation and electron-phonon coupling, the connection between finite and infinite wires is not straightforward in CAWs. In fact, starting with the infinite structure, two arrangements of the C atoms within the unit cell are possible (Fig. 2).

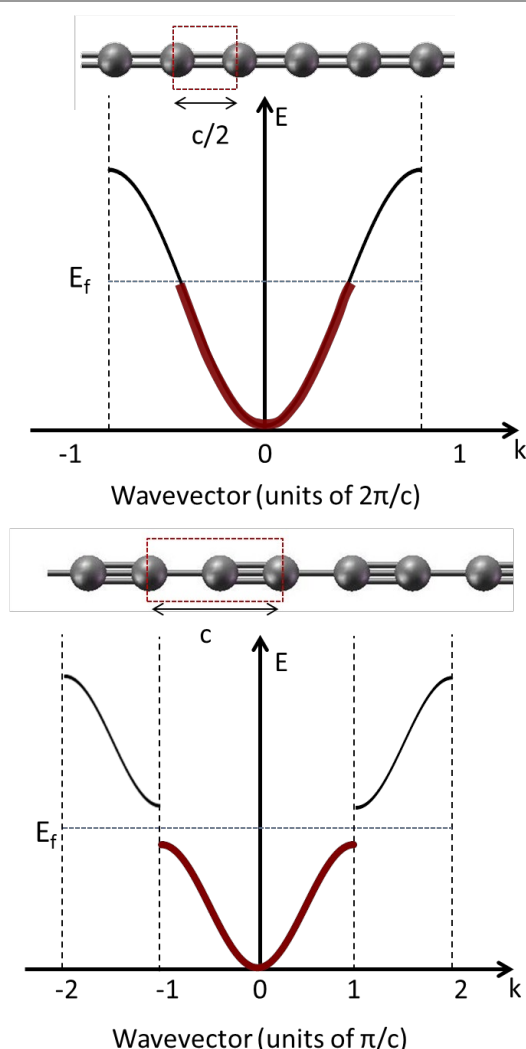


Figure 3. Sketch of the two possible geometric arrangement of the infinite CAW (i.e., carbyne) with the corresponding band structure according to a solid-state physics approach: equalized double-bond structure (polycumulene, top), alternate quasi simple-quasi triple bonds (polyynene, bottom). The band filling reveals the metal and semiconducting character of cumulene and polyynene, respectively.

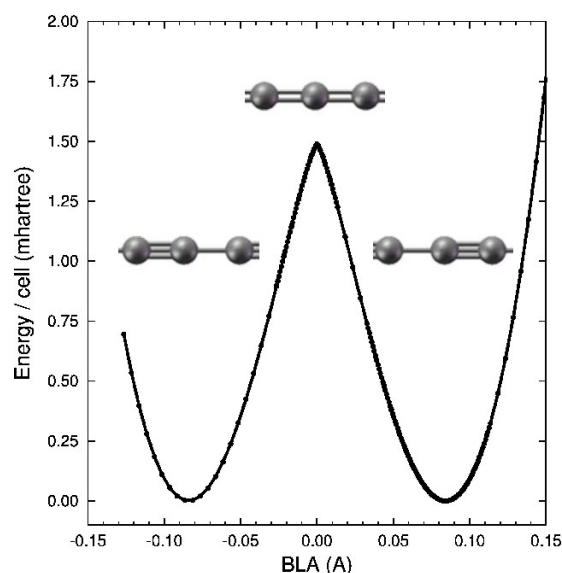


Figure 4: Potential energy surface of an isolated infinite linear carbon chain as a function of BLA, as obtained by periodic boundary conditions calculations,⁵⁹ showing the occurrence of Peierls distortion (instability of the equalized, cumulene-like geometry) and the stabilization of the two possible (and equivalent) bond alternated (polyynene-like) structures.

One structure consists of equivalent (equalized) double bonds. This is referred to as polycumulene (or simply cumulene) and it can be described as a 1-D crystal with a monoatomic unit cell. The other arrangement is characterized by a sequence of alternating triple and single bonds (polyynene). The polyynene form corresponds to a 1-D crystal with a unit cell containing two carbon atoms. Cumulene is a metal since the conduction band is half filled (one carbon atom contributes with one electron for each of the two 2p orbitals). In polyynes, however, the double unit cell provides two electrons in each orbital and results in a half Brillouin zone. Hence, the valence band is completely filled by electrons while the conduction band, separated by the band gap opened at the edge of the Brillouin zone, is empty thus leading to a semiconductor (Fig. 3). Due to π -electron delocalization, the CC bond lengths of the infinite polyynene are not exactly those of an ordinary triple and a single CC bond (*e.g.*, that of acetylene or ethane). Actually the triple bonds are slightly longer than in acetylene (ca. 1.2 Å) and the single bonds are slightly shorter than in ethane (ca. 1.5 Å). A useful parameter to define the wire structure is bond length alternation (BLA), which is the difference in bond lengths for adjacent bonds (typically measured at the centre of the molecule). BLA is non-zero in polyynene,⁵⁶ and it is ideally zero for cumulene. As in the case of a linear metal and other polyconjugated materials (*e.g.*, polyacetylene), CAWs are affected by Peierls distortion,^{57,58} which states that cumulene is unstable upon a change in BLA and undergoes a transition to the alternated, polyynene-like configuration that corresponds to the minimum energy. This is illustrated in Fig. 4 by the potential energy curve plotted as a function of BLA, as obtained by quantum chemical calculations.⁵⁹

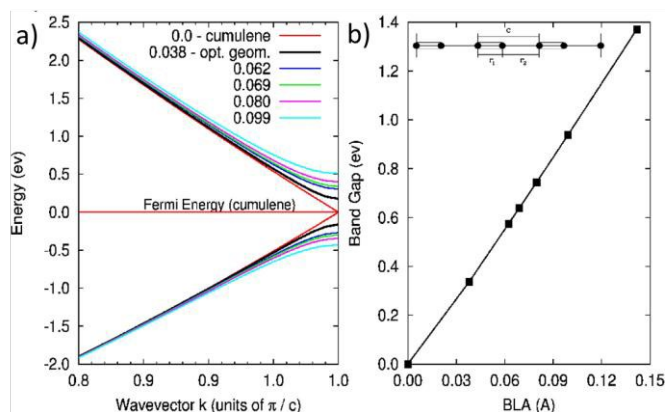


Figure 5: a) Band structure of a carbon atomic wire for cumulene (BLA = 0) and for different values of BLA in Å (ideal polyne with optimized geometry shows a BLA = 0.038 Å); adapted with permission from ref. 54, copyright 2006 by the American Physical Society. b) band gap as a function of the BLA. The wire structure and definition of BLA as $r_2 - r_1$ is also shown.

BLA significantly affects the electronic structure of the sp-carbon chain, driving the transition from a metallic to a semiconducting system, which influences both the optical and vibrational properties. This transition is illustrated by the electronic band structure of ideal CAWs as a function of BLA (Fig. 5) resulting from DFT pseudopotential calculations.⁵⁴ As required by Peierls distortion, the equilibrium geometry has $BLA \neq 0$, corresponding to a finite band gap. The band gap widens for increasing BLA, while it decreases for smaller BLA. In the limit of small BLA, π -electron conjugation is enhanced, i.e., the electrons are more effectively delocalized along the chain, until the metallic character is actually reached in cumulene (BLA = 0). As a consequence of Peierls distortion, only polyne chain represents the minimum energy configuration leading to a well-defined BLA value (i.e. corresponding to optimized geometry). Other cases obtained by imposing a different geometry may represent convenient models to investigate the effects of modulating the BLA. In fact, when relaxing the infinite chain approximation, we will see that endgroup effects, charge transfer, and photoexcitation processes, etc. are all effective ways of modulating the BLA. Hence, real systems (finite length CAWs) can be correlated with the appropriate model of an infinite chain possessing the same BLA. The possibility of inducing, by means of chemical or physical processes, an effective modulation of the molecular structure that can control the electronic properties is very appealing from the point of view of the possible applications of CAWs in technology.

Due to the well-known electron-phonon coupling that exists in all π -conjugated systems, it is reasonable to expect that changes in BLA might also significantly influence the vibrational properties of CAWs. This motivates the use of vibrational spectroscopy (IR and Raman) as a sensitive method for characterization of sp-carbon wires (see Section 2.3).

In order to discuss the vibrational structure of CAWs, it is useful to refer to the limiting case of the infinite linear carbon chain. Considering cumulene first, the description of its phonon dispersion is elementary and constitutes a classical

textbook example for introducing the concept of phonons in a monoatomic infinite chain as a 1-D crystal.⁶⁰ Cumulene displays only acoustic phonon branches (one longitudinal acoustical, 1LA and 2TA, respectively), and the system would not present any optical activity.^{57,60} The polyne case corresponds to a homo-atomic chain with different bond strengths so that the unit cell is composed by two atoms. As a result, there are three acoustic and three optical phonon branches (Fig. 6). In other words, upon moving from cumulene to polyne the major effect is the appearance of optical phonon branches. This matter has been considered in the literature to exclude the possibility that cumulene-like sp-carbon wires might not be observed by Raman or IR spectroscopy. While this is certainly true for infinite cumulene, for finite length CAWs this selection rule must be relaxed, since endgroups play a role, i.e., BLA is affected by the terminal endcapping groups, and the spectroscopic behaviour of finite-length cumulenes will deviate from the infinite chain model.⁶¹

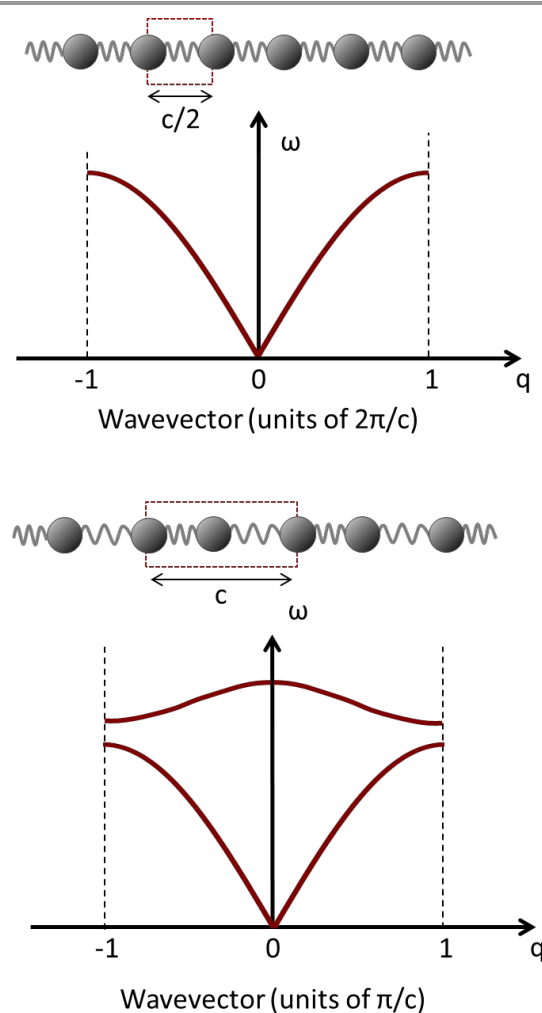


Figure 6: Sketch of the phonon dispersion branches of a bond equalized (cumulene, top) and alternate (polyne, bottom) infinite wire (i.e., carbyne as 1-D crystal).

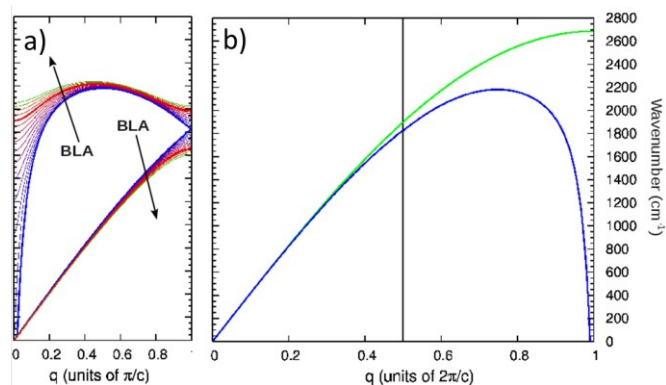


Figure 7: Phonon dispersion relation for wires as a function of BLA. (a) Longitudinal Optical (LO) and longitudinal acoustic (LA) phonon dispersion branches of an infinite polyene (adapted with permission from ref. 55; copyright 2008 AIP Publishing LLC). (b) Comparison between phonon dispersion of a carbon-atom wire with (green line) and without (blue line) nearest neighbour approximation.

The phonon dispersion of the longitudinal optical (LO) branch has been computed for polyynes with varying BLA by means of a tight-binding model that couples the vibrational force field (i.e., the dynamical matrix) to the expected changes of the electronic structure.⁵⁴ This approach corresponds to solving the vibrational dynamics of the CAW subjected to a constant external force that sets the BLA as desired. As shown in Fig. 7, the LO branch depends dramatically on BLA: the phonon wavenumber at $q = 0$ ranges from 1200 to more than 2000 cm^{-1} for increasing BLA in the range 0.038–0.142 Å.⁵⁴

The over bending of the phonon dispersion and the softening of the phonon in the vicinity of $q = 0$ is due to long-range vibrational interactions along the chain^{55,62} (i.e., the inclusion in the harmonic potential of interactions beyond the nearest neighbour approximation).⁵⁷ The strength of long-range interactions increases as the system approaches the structure of cumulene, and the electronic structure evolves from semiconducting to metallic. In fact, similarly to graphite⁶³ and carbon nanotubes,^{64,65} cumulene is affected by a Kohn anomaly⁵⁴ that makes the phonon dispersion divergent at the Γ point (in reciprocal space of polyene).

As shown in Fig. 7b, which depicts the acoustic phonon branch of cumulene, if one considers only nearest neighbour interactions in the harmonic potential, one can fit only the frequencies close to the Γ point, where the Kohn anomaly effects are negligible. This approximation breaks down at the first Brillouin zone boundary, which shows that the Kohn anomaly is due to effects beyond the nearest neighbour approximation and may also require inclusion of anharmonicity.¹¹ It is important to note that by taking the description of cumulene with a translational unit comprised of two carbon atoms (Fig. 7a), the Kohn anomaly is found at $q = 0$, otherwise it is found at the Brillouin zone boundary (Fig. 7b). To gain better insight into the vibrational properties of CAWs, it is worth introducing some additional theoretical details, which are based upon theories introduced to deal with the vibrational spectroscopy of π -conjugated polymers.⁶⁶⁻⁷⁰ In this field, Raman spectroscopy certainly plays a major role (see for instance refs. 71-75 and refs. therein). The Raman spectra of π -

conjugated polymers are usually dominated by intense Raman lines, which are related to BLA oscillation. These lines show sizeable frequency and intensity dispersion with chain length. For increasing chain length the Raman signal associated with BLA oscillation shifts to lower wavenumbers and becomes more intense. This behaviour has been rationalized by means of two theories, the “amplitude mode theory” (AMT)⁷⁰ and the “effective conjugation coordinate” (ECC) model.⁷¹⁻⁷⁴ These two approaches are rigorously related one to the other (see Milani et al.^{55,71}). According to the ECC model, the normal mode associated to the most intense Raman line has been named the “ECC mode” and it has found applications in the interpretation of the Raman spectra of many different π -conjugated oligomers and polymers. Unlike oligomers and polymers, as well as forms of carbon (e.g., graphite, diamond, fullerene, nanotubes), Raman analysis of sp-carbon chains has been investigated only recently in detail. Since polyynes/cumulenes are π -conjugated systems, the concepts developed in the AMT or the ECC model can be applied successfully. For infinite polyene, the LO phonon at $q = 0$ can be regarded as a stationary wave in which the CC bonds r_1 and r_2 simultaneously oscillate out-of-phase in the entire crystal. Hence the nuclear displacements associated with the LO phonon can be regarded as a collective BLA oscillation corresponding to the ECC mode. The frequency associated to this phonon can be analytically determined in terms of bond stretching force constants,^{54,55,57,76} effectively demonstrating the role of long-range interactions in determining the marked frequency decrease in the phonon dispersion (at $q = 0$) as BLA approaches zero. This calculation can be conveniently carried out by adopting the infinite chain model with a unit cell of length c containing two carbon atoms and by following Wilson’s GF method⁷² generalized to periodic systems:

$$\mathbf{G}(\theta)\mathbf{F}(\theta)\mathbf{L}(\theta) = \mathbf{L}(\theta)\mathbf{\Lambda}(\theta) \quad (1)$$

where $\theta = qc$, \mathbf{G} is the kinetic energy matrix, \mathbf{F} collects the valence force constants, \mathbf{L} describes the normal mode displacements along the internal coordinates (e.g., CC stretchings) and $\mathbf{\Lambda}$ is the diagonal matrix that collects the phonon frequencies ($\lambda_i = \omega_i^2$) at a given θ (the index i labels the different phonon branches). The following solution is obtained for the LO phonons in correspondence of $q = 0$:^{54,55,71}

$$\omega^2 = \frac{4F_R}{m}; \quad F_R = \frac{k_1+k_2}{2} + \sum_{n \geq 1} [f_1^n + f_2^n - 2f_{12}^n] \quad (2)$$

In Equation (2), F_R is defined on the basis of several terms: k_1 and k_2 are the diagonal stretching force constants relative to the two bonds (r_1 , r_2) within the cell, and the various f_n terms describe interaction stretching force constants at increasing distances (n) along the chain. The variables f_1^n and f_2^n are associated to the interactions between equivalent bonds belonging to different cells; f_{12}^n describes the interaction between non-equivalent bonds at distance n . Equation (2) demonstrates that π -conjugation effects in CAWs are qualitatively similar to those occurring in other π -conjugated systems. For instance, it has been verified that the sequence

the interaction stretching force constants involving a given CC bond and a sequence of bonds along a path made by consecutive CC bonds have alternate signs in polyynes,^{55,62,73} similarly to polyenes and graphene.^{52,67-69,74} As a consequence, the sum in Eq. (2) has a negative value. This provides a π -conjugation-dependent contribution that lowers the phonon frequency with respect to the value given by the diagonal force constants k_1, k_2 . This decrease of F_R for increasing π -conjugation is responsible of the frequency dispersion of the intense Raman line associated to the ECC mode, which matches the behaviour at $q = 0$ shown in Fig 7a.

The physical origin of this phenomenon is the electron-phonon coupling typical of these systems, even in presence of π -electron delocalization. A simple model based on Hückel theory (*i.e.*, tight binding restricted to π -electrons) can be introduced to better quantify these effects,^{55,62,71} leading to the following formulation of the matrix elements of the F matrix of CC stretching force constants:

$$F_{ij} = \delta_{ij}k_i^{\sigma} + 4\left(\frac{\partial\beta}{\partial r}\right)^2 \Pi_{ij} \quad (3)$$

Π_{ij} are the bond-bond polarizabilities and $\partial\beta/\partial r$ is the electron-phonon parameter, with β the hopping integral of Hückel theory. This model allows relating the electronic and vibrational properties, predicting the observed modulation of the electronic bands and phonon dispersion branches (Fig. 8), also in a good agreement with quantum chemical calculations.⁵³ The model also allows for introduction of the correlation that exists among BLA, LO phonon wavenumber, and band gap in CAWs, which formally defines the connection between structural, electronic, and vibrational properties.⁷¹

The infinite chain model provides a reliable interpretation of experimental data and captures the main trends observed for the electronic and vibrational properties, thus offering a useful unified framework for the understanding of real systems.

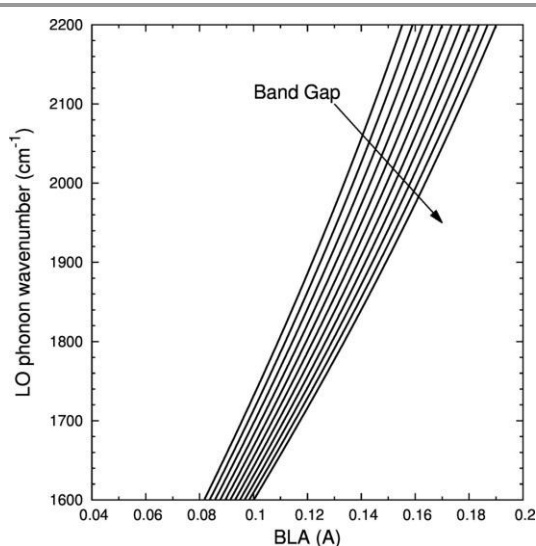


Figure 8: Correlation between the LO phonon wavenumber (ECC mode) and bond length alternation BLA for different values of the electronic band gap, as obtained on the basis of Hückel theory applied to the linear infinite carbon chain.^{55,71}

However, the use of periodic boundary conditions along the chain axis has a non-negligible influence on the spectroscopic selection rules: deviations of the chain structure from linearity,⁷⁵ endgroup effects,^{61,76} and Peierls distortion (cumulene vs. polyyne) in long C_n wires require relaxing the infinite chain model, as described in the next section.

2.2 Finite length sp-carbon systems: BLA and π -electron delocalization

Moving from ideal (*i.e.*, infinite chain) to real (*i.e.*, finite length) structures, endgroup effects play a leading role: the chemical nature of the endgroups influences the overall structure of the chain, increasing or decreasing BLA and, thus, modulating the energy gap and vibrational properties of the chain. The possibility of actually tuning the electronic properties and the conducting character by proper functionalization could be the key point for future technological applications, such as the realization of nanoscale cables and devices that have been proposed in theoretical studies.^{9-11,77}

CAWs of increasing length show a decreasing BLA as a result of increasing π -conjugation.^{54,73,78-81} However the BLA = 0 limit (cumulene) is not reached due to Peierls distortion. In this framework, the alternate (polyyne-like) structure found in most of the synthesized sp-carbon wires⁵⁶ has been usually interpreted as the result of Peierls distortion, as also reported for other classes of π -conjugated materials. However, such an interpretation is prone to some criticism due to the fact that Peierls distortion is an effect that can be defined just for the infinite chain, not for relatively short CAWs for which the end functional groups are certainly stronger agents in determining BLA (see below).

A detailed computational analysis on long uncapped cumulene-like C_n wires clearly demonstrates that Peierls distortion becomes effective only in very long chains ($n > 52$), where it can overcome the BLA decrease driven by π -electron delocalization.⁸¹ As a result of the balance between π -electron delocalization and Peierls distortion, C_n wires possess a cumulene-like structure (determined by endgroup effects) for $n < 52$. Longer C_n wires exhibit an alternated, polyyne-like structure due to the onset of Peierls distortion. This provides the evidence that Peierls distortion may be rigorously defined just for an infinite chain and might not effectively explain the molecular structure observed in short CAWs. For these wires the presence of endgroup effects is essential^{80,81} and the carbon chain structure is mainly determined by the chemical nature of the endgroups, as highlighted by the values of BLA and CC bond lengths reported in Fig. 9 for a few series of sp-carbon molecules.⁶¹ In hydrogen endcapped wires, the CH single bonds require the presence of a triple bond on the adjacent CC linkage, so that a single bond is formed on the next CC and so on, thus inducing a polyyne-like structure. However, a vinylidene endgroup (*i.e.*, =CH₂) induces a CC double bonds at the termini of the sp-chain, resulting in a more equalized cumulene-like structure.

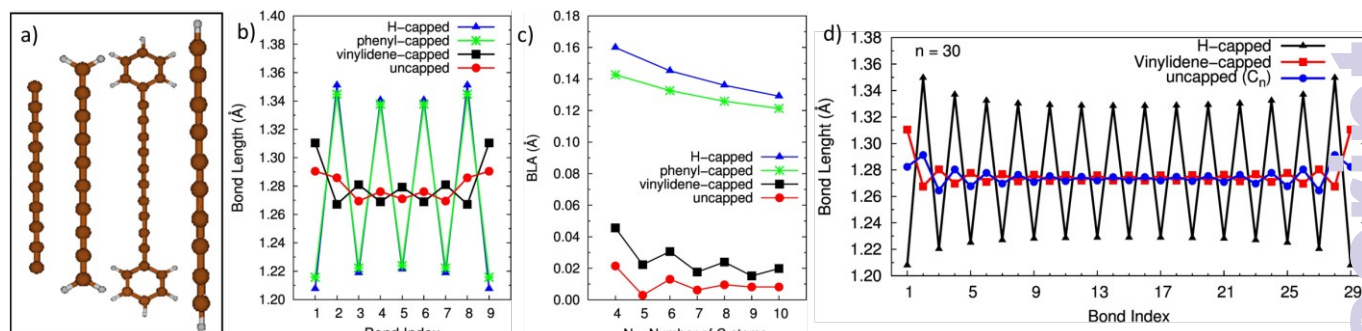


Figure 9: (a) structure of the considered wires (from left to right): uncapped, vinylidene-, phenyl- and H-terminated; (b-c) Bond length and bond length alternation (BLA) as a function of the number of carbon atoms for different types of wires. (d) bond lengths in long wires (*i.e.*, 30 carbon atoms) with different terminations.. Data are from DFT calculations. Adapted with permission from ref.8

Hence, for the same number of C atoms in the sp-chain, vinylidene endgroup results in a substantially smaller BLA with respect to hydrogen endgroups. Clearly, this behaviour facilitates the design of new sp-carbon compounds with tunable properties by means of a proper choice of the endgroups and synthetic approach. An example of this approach is represented by the recent work by Tykwinski et al.^{82,83} where long cumulene-like CAWs (up to 9 C=C bonds) have been obtained by rational chemical synthesis. It should be noted that in finite-length wires, the cumulene-like geometry does not correspond to the ideal case with BLA = 0. Finite cumulenes are systems showing small BLA values, which are markedly different from those found in polyynes. A further demonstration of the significance of finite length effects is given in Fig. 9d, which shows the bond lengths of quite long wires (30 carbon atoms) with different endgroups: CAWs still display very different CC bond lengths and BLA. Hence for these CAWs it is primarily the chemical nature of the end-caps that determines structure, not the length of the chain. However, for fixed endgroups, BLA decreases with chain length until it reaches an asymptotic lower limit, as generally expected by increasing π -conjugation.^{54,61,73,78-81,84}

Based on the concepts illustrated above, a strict one-to-one correspondence between the infinite wire (*i.e.*, carbyne) and finite-length CAWs cannot be established. However, due to the variance in BLA observed in CAWs as a function of length and/or endgroups, finite CAWs should be related to different reference wire models possessing the same BLA as their finite counterpart. For instance, considering the electronic properties of finite CAWs, it becomes straightforward to suggest that by increasing chain length (or by the proper choice of endgroups), the sp-chain will be characterized by a smaller BLA values, leading to a smaller optical gap and a larger wavelength of the associated absorption band. This has been observed in many different CAWs, which also demonstrates the importance of spectroscopy as a quick and effective method for characterizing the structural properties of these systems. However, the absorption wavelengths observed in finite wires should be considered with care before extrapolating the electronic properties of the infinite polyynes. This is due to the fact that different finite-length CAWs are potentially associated to parent systems with different BLA.

Extrapolation procedures have been discussed in some work^{34,83}

2.3 Finite length sp-carbon systems: molecular vibrations and Raman spectroscopy

Parallel to the case of the electronic properties, where finite length CAWs can be put in correspondence with an infinite chain model sharing the same BLA (see Section 2.2), an analogous correlation should also be worked out for the vibrational properties of CAWs. The Raman spectra of hydrogen-terminated polyynes show a similar pattern as polyenes, namely a very intense line that corresponds to the ECC mode,^{75,86} and this has been also named “ α -line” in the literature.⁸⁷ A second minor band (β -line) is often observed notably in shorter H-terminated polyynes.⁵⁴ These Raman signals fall in the 1800-2300 cm^{-1} spectral region. Through theoretical analysis and first-principles calculations it has been possible to assign the α - and β -lines to different collective stretching vibrations of CC bonds (*i.e.*, BLA oscillation modes).⁸⁷ This spectral region turns out to be specific for sp-carbon: no other carbon nanostructure shows any Raman signal in this region (Fig. 10).

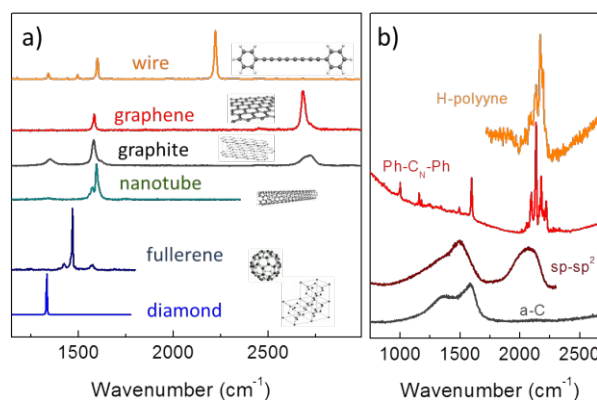


Figure 10: (a) Experimental Raman spectra of carbon solids and (b) carbon-based nanostructures.

In fact, the Raman spectra of sp^2 -based carbon nanostructures show a maximum frequency of about 1620 cm^{-1} that corresponds to the maximum in the phonon dispersion of graphite. All the other features appearing above 2400 cm^{-1} are due to II order Raman scattering, including the 2D peak whose intensity and shape is peculiar in graphene.

Similarly, the Raman peak of diamond at 1332 cm^{-1} represents the highest frequency in the phonon density of states. Hence, the Raman modes of CAWs appear in a spectral region where no other carbon systems show characteristic peaks.

Based on the results predicted for ideal carbyne^{54,55,62} and the general properties of polyconjugated molecules, the red shift of the most intense ECC Raman line observed when increasing the chain length has been qualitatively and quantitatively interpreted as a manifestation of large electron-phonon coupling. To this aim, DFT calculations on finite length CAWs proved to be very helpful for the spectroscopic characterization of these systems.^{55,59,61,73}

A first interpretation of the Raman spectra of real sp -carbon wires can be carried out by taking into account the infinite chain model which allows to interpret the α - and β -lines on the basis of the LO phonon dispersion branches of carbyne, where the semiconductive-metallic transition (as $BLA \rightarrow 0$) involves the appearance of a Kohn anomaly at Γ in the case of a cumulene-like chain.^{54,55,59,62,73}

As mentioned above (Section 2.2), collective CC stretching vibrations of CAWs involve stretching of triple and single bonds, which give rise to Raman and IR signals in the range of $1800\text{--}2200\text{ cm}^{-1}$, depending on the length of the chain.^{28,75,76,87}

In order to classify the CC stretching vibrations of finite chains by establishing a correspondence with the LO phonon of the infinite polyyne, it is useful to adopt a procedure successfully employed in the past for the study of the vibrational dynamics of crystalline polymers.^{48,50} This procedure consists in selecting the suitable value of phonon wavevectors (q) for which the vibrational wavenumbers of the oligomers can be placed as discrete points on the phonon dispersion curves of the corresponding carbyne (with proper BLA). It has been shown that these discrete q values are given by the formula:^{48,73}

$$q_j = \frac{\pi}{c(N+1)} j; \quad j=1,2,3,\dots \quad (4)$$

where N is the number of unit cells which can be devised in the finite chain (oligomer).^{48,50} Provided that endgroup effects have a limited influence on vibrational dynamics (which is often an accurate approximation for long enough oligomers), the procedure yields an accurate description of the normal modes which can be related to a given phonon branch.

In Fig. 11 this procedure has been applied to the longitudinal vibrations of the hydrogen-endcapped polyyne containing seven triple bonds.⁷³ The vibrations of the molecule have been put on the (LO, LA) phonon dispersion of the infinite polyyne.

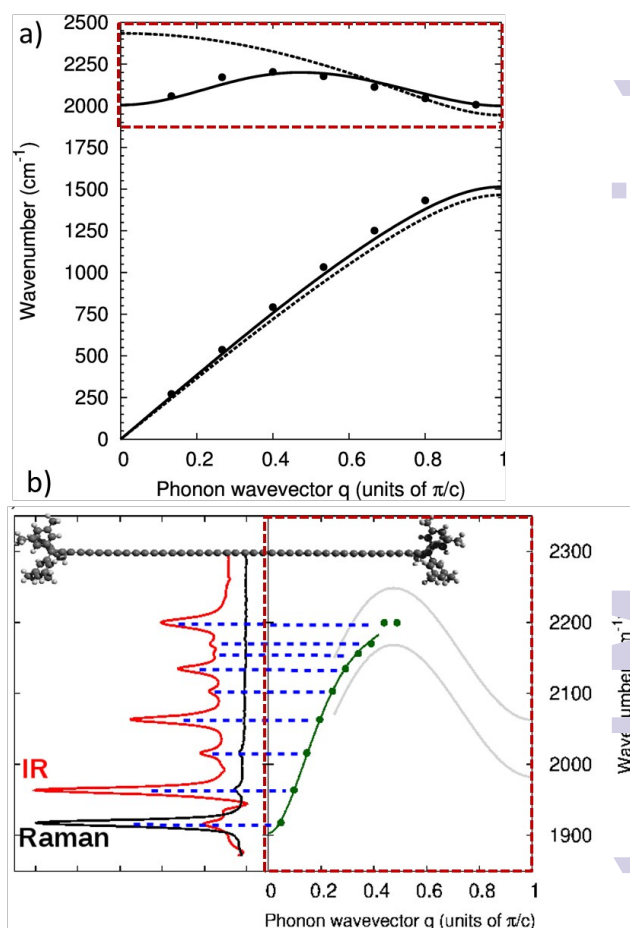


Figure 11: a) LO and LA phonon dispersion curves (full lines) obtained by using the DFT computed vibrational force field of a finite-length (7 triple bonds) Hydrogen-endcapped polyyne.⁷³ Black dots represent how the vibrational frequencies for this wire can be located on the phonon dispersion branches (see discussion in the text). For comparison, the phonon curves obtained by removing all long-range interactions (f_n terms in eq (1)) are reported as dashed lines. Reprinted with permission from ref. 73, copyright 2007 American Chemical Society. b) The same LO plot has obtained on the basis of IR and Raman measurements carried out for a long polyyne endcapped with super-trityl groups (super-trityl = tris(3,5-di-*t*-butylphenyl)methyl).⁷⁶

The phonon dispersion was computed by using Wilson's approach (eq. 1,2) and by considering the force field F taken from the oligomer (*i.e.*, considering the central triple bond of the finite chain as the reference 0-th cell of the polymer and interactions up to the edge of the molecule). In non-conjugated polymers the oligomer-polymer correspondence can be established by considering just one oligomer long enough to minimize endgroup effects.

All longer oligomers can be related with that phonon dispersion. In contrast, each π -conjugated oligomer is characterized by a different degree of conjugation (hence different BLA). In principle, this implies that each oligomer possesses a different force field and leads to a different oligomer-derived phonon dispersion. From the experimental point of view, IR and Raman measurements carried out for a long super-trityl -endcapped polyyne have provided several CC stretching signals (Fig. 11).⁷⁶ The assignment of these IR and Raman features by DFT calculations allows drawing the corresponding phonon dispersion relation.⁷⁶ This shows that

the relationships qualitatively follows theoretical expectations,^{54,73} and it exhibits the behaviour represented in Fig. 7 (left panel). In other words, the properties of finite-length CAWs can be related to that of the carbyne possessing the appropriate BLA for phonon dispersion branches. This model has been successfully adopted to give an interpretation of the Raman spectra of hydrogen-encapped CAWs of increasing lengths^{54,73} and long polyynes (containing up to 20 conjugated triple bonds) encapped with bulky groups.⁷⁶ The strong Raman line (ECC mode) that is found on the LO dispersion corresponding to $j = 1$ for long wires is essentially equivalent to the $q \approx 0$ phonon.^{54,73,76} In finite polyynes, IR modes are observed for values $j > 1$, and these can be simply considered as higher “harmonics” of the Raman active $j = 1$ mode (see Fig. 11).^{75,76}

The dependence of the vibrational properties on BLA makes the interpretation of the Raman spectra a non-trivial issue, requiring the support of numerical simulations. Chain conformation effects on the Raman spectrum have also been studied both experimentally and theoretically.^{75,76,79,88} These works show that first-principles calculations can be helpful to elucidate the connections among structural, vibrational, and electronic properties of sp-carbon chains. Yang et al.⁸⁰ and Tommasini et al.⁷³ have analysed the relationship between BLA of hydrogen-encapped polyynes and their Raman response, by means of DFT calculations.

The connection between the properties of finite-length CAWs and the ideal infinite polymers was characterized in different works by using DFT calculations^{54,73} or tight-binding models,^{55,62,71,85} reconciling the approaches usual found in the Physics and Chemistry communities. The same methodologies were applied to the characterization of new synthetic series polyynes bearing suitable endgroups.^{75,89}

The subtle problem of the existence of cumulene-like species and their detection by means of vibrational spectroscopy has been also addressed.⁶¹ This case is particularly interesting since it shows the inherent limits of the infinite chain model. In the literature, in fact, the possibility of observing cumulene-like wires by Raman spectroscopy has been contrasted by some authors<<not sure how to fix this, since I'm not sure what you meant to say>> based on the assumption that, as in model cumulene, they do not possess any optical phonon branch. However, Raman signatures of the existence of cumulene-like species have been suggested for mixed sp/sp²-carbon nanostructures.^{27,88,90} This supposed controversy can be solved by relaxing the “carbyne perspective”. At difference with a model system (i.e. 1-D crystal) for which only phonons at Γ could possess Raman activity, for finite wires also vibrations located on the LO branch at different points of the first Brillouin zone can be Raman active. This may happen as a result of endgroup effects, which constitute a perturbation over the strict periodic boundary conditions scheme introduced above.

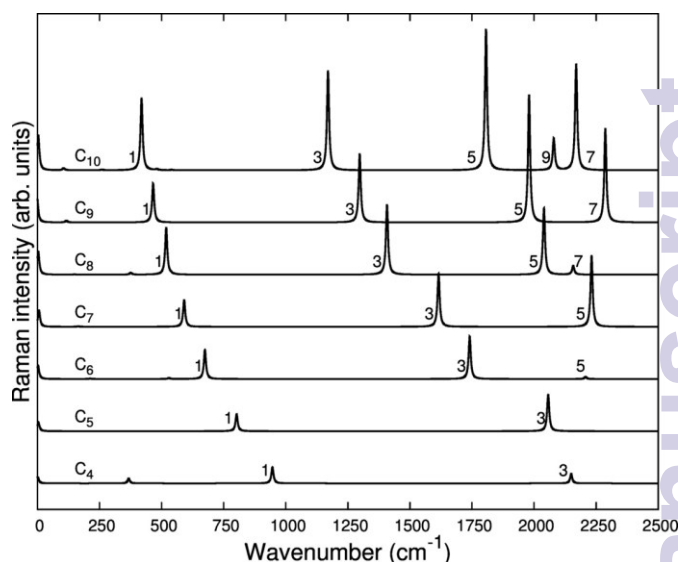


Figure 12: Calculated Raman spectra of cumulene-like C_n chains of different lengths. Bands are marked with labels indicating the number of nodes of the associated atomic displacements. Reprinted with permission ref. 61, copyright 2009 John Wiley and Sons.

The Raman spectra of several cumulene-like wires (C_n) have been predicted by means of DFT calculations,⁶¹ and, interestingly, many vibrational transitions show non negligible Raman intensity, which demonstrates the possibility of detecting finite length cumulene-like wires by means of Raman spectroscopy. The reason for this behaviour lies in the interplay between the activation of out-of- Γ normal modes and the molecular parameters governing Raman activity.⁷¹ This originates in cumulenes a detectable Raman signal for LO modes other than ECC, as shown in Fig. 12. The Raman intensity of a given line is related to the square of the derivative of the polarizability tensor with respect to the associated normal mode Q_k . This parameter can be written in terms of bond contributions as follows:

$$\frac{\partial \alpha}{\partial Q_k} = \sum_i \frac{\partial \alpha}{\partial R_i} * L_{ik} \quad (5)$$

L_k is the eigenvector describing the normal mode Q_k on the basis of internal valence coordinates (CC stretching, R_i) and $\partial \alpha / \partial R_i$ are polarizability derivatives with respect to the individual CC stretching (R_i) along the chain.⁹¹ In a cumulene, the $\partial \alpha / \partial R_i$ parameters are all very similar due to the similar character of all the CC bonds. The ECC mode describes the in-phase shrinking ($L_{ik} < 0$) and stretching ($L_{(i+1)k} > 0$) of adjacent CC bonds (R_i and R_{i+1}): therefore, almost equal $\partial \alpha / \partial R_i$ in the sum of Eq. 5 are weighted by L_{ik} values of opposite sign. This results in a vanishing sum, implying that the ECC mode has a small Raman intensity. This result is consistent with the infinite carbyne model. However, the infinite chain model cannot take into account the fact that other LO modes (out of Γ) have a different L_k vector than the ECC mode.

This implies that the sum in Eq. 5 can have a non-negligible value and the associated Raman lines may be detectable, as shown in Fig. 12 and described in ref. 61. Thus this discussion about cumulenes has a twofold meaning. On one hand,

demonstrates the possibility of the spectroscopic detection of cumulene-like wires; on the other hand it reveals that in finite CAWs (real systems), some phenomena can be straightforwardly understood by only relaxing the infinite chain approximation. Based on the above discussion, it should be clear that endgroup effects might influence the overall properties of sp-carbon wires, *i.e.*, by modifying the molecular structure (BLA) that affects the electronic and vibrational properties. Therefore, by selecting endgroups one can modulate the properties of the chain, which might be probed by spectroscopy thanks to the evolution of the distinct marker bands observed in the Raman (or IR) spectra. In this context, Raman spectroscopy, supported by first-principles simulations, proves to be a powerful non-invasive characterization technique that can provide valuable information on the molecular properties of sp-carbon systems and can be useful in nanotechnology application scenarios.

In Section 4 we introduce a few recent case studies in which vibrational spectroscopy provides to be particularly insightful to characterize sp-carbon systems with peculiar and not standard behaviour. For specific systems, we will show that Raman spectroscopy allows the identification of CAWs with different lengths, and we will highlight the observance of peculiar intra- and intermolecular effects.

3. Synthesis and preparation of sp-carbon systems: a brief overview

Today, many techniques can be found in the literature for the synthesis of sp-carbon systems. The different techniques are based on both physical and chemical strategies mainly in a bottom-up approach.^{22,92,93} Techniques based on physical vapour deposition methods depend on the production of a carbon vapour or plasma that is rapidly quenched to induce clustering of carbon atoms in out-of-equilibrium conditions. The carbon vapour can be produced by arc discharge or laser ablation, and the quenching can be accomplished by the use of inert gas molecules or liquids. We mention supersonic cluster beam deposition (such as the pulsed microplasma cluster source – PMCS developed by P. Milani and co-workers),⁹⁴ laser vaporization methods^{95,96} and femtosecond laser ablation of graphite.⁹⁷ These techniques typically produce solid samples in the form of thin films on substrates. The deposited material is usually composed of sp-sp² moieties where sp-wires are mixed in a mainly sp²-amorphous carbon matrix (sp-content up to 40% has been estimated in some cases).⁹⁸⁻¹⁰⁰

Laser ablation (with both fs and ns pulses) of solid carbon targets or suspensions (e.g., fullerenes, nanodiamond) produces solutions of isolated wires in the form of polyynes with an even number of carbon atoms.^{101,103} An easy-to-use and cost-effective technique for the synthesis of polyynes in solution is the arc discharge in liquids developed by F. Cataldo.¹⁰³ This technique also allows one to control the chain termination by selecting suitable solvents.¹⁰⁴

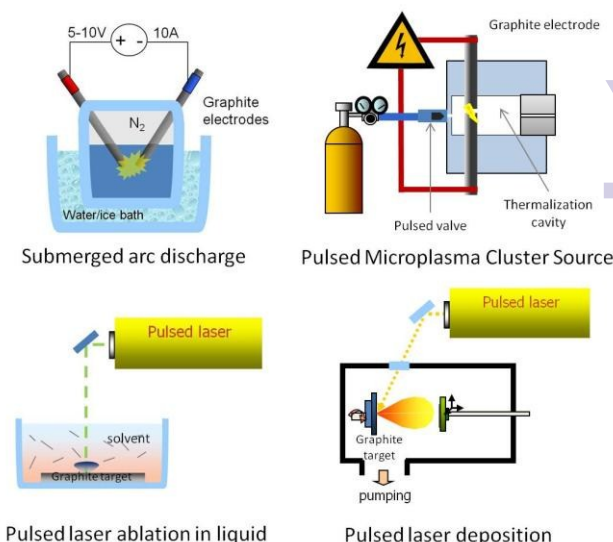


Figure 13: Sketches representing several known physical methods adapted to synthesize linear sp-carbon wires. Reprinted with permission from C.S. Casari Istituto Lombardo (Rend. Scienze) 2012, 146, 17-35 [eISSN 2384-986X].

Chemical synthesis has been often used to synthesize systems in solution. Two approaches are often pursued. The first employs a polymerization strategy, as has been reviewed by Kudryavtsev.^{105,106} These syntheses are based on, for example, dehydropolycondensation of acetylene, polycondensation reactions of halides, dehydrohalogenation of polymers, or chemical carbonization of poly(vinylidene halides). In these cases, the resulting sp-carbon wires can be efficiently formed in a single step, but the products are polydisperse due to the nature of the synthetic protocol. Furthermore, solution state characterization of the resulting product is often challenging. The second approach targets molecules with defined length and endgroup constitution, typically via the dimerization reaction of ethynyl groups (Glaser reaction),¹⁰⁷ with defined length and specific endgroups, and salient examples can be found in reviews by Szafert and Gladysz,⁹³ Jevric and Nielsen and Chalifoux and Tykwinski.^{108,109} In these cases, a homologous series of molecules can be made and studied as a function of length, allowing prediction of properties of carbyne, as well as molecules that are not yet synthetically assessable.

Polyynes can also be formed on a surface, such as the formation of Pt-endcapped wires has been observed by TEM on graphene where Pt atoms act as nucleation sites of additional carbon atoms.¹¹⁰ TEM has been used to obtain wires suspended between graphene sheets in a top-down approach. The electron beam has been controlled to selectively remove carbon atoms from a graphene layer until a single atomic chain connecting two separate graphene edges was obtained and imaged.¹¹¹ Other top-down methods are based on pulling carbon nanotube or graphene in order to form a wire as predicted by theoretical studies.

Stability is a key issue in the synthesis of wires (**Caution:** *the isolation of sp-carbon wires in the solid state should always be done with extreme care, since explosions are possible*

especially in the case of H-terminated polyynes).²¹ Cross-linking reactions of polyynes in the solid state play a lead role in reorganization processes of sp-wires towards amorphous sp²-carbon. To overcome this problem, one possibility is to stabilize already formed wires. Some strategies of this kind have been proposed so far. H-Terminated polyynes produced by submerged arc discharge in water show reduced stability,^{86,112} while mixing the solution with silver colloids results in a prolonged stability even in the solid state. In fact, by simply drying the solution one can obtain a solid sample (e.g., a thin film) consisting of an assembly of silver nanoparticles in which wires display stability under ambient conditions for several weeks.¹¹³ A similar system of wires stabilized by silver can be also used to produce a nanocomposite, as showed by Hayashi and co-workers using poly(vinyl alcohol) as a polymeric matrix.¹¹⁴ An alternative strategy consists in designing and incorporating endgroups at the termini of the wire during the synthesis, for example sterically bulky groups, in order to prevent intermolecular wire-wire interactions and subsequent cross-linking. Stable samples in powder form have been produced,¹¹⁵ as a chief example Chalifoux and Tykwinski synthesized long wires (44 carbon atoms) stabilized by bulky endgroups.³⁶

Polyynes are typically easier to produce than cumulenes probably due to a higher stability, and nowadays polyynes up to 20 carbon atoms and more can be produced in solution even as size-selected samples.^{22,28,75} Step-wise syntheses offer the possibility of different terminating groups.⁹³ On the other hand, cumulenes are more difficult to produce and there are far fewer reports of their synthesis and study in the literature. Cumulene-like structures have been observed together with polyynes in a pure sp-sp²-carbon cluster-assembled system.^{27,88} It has been observed that the cumulene fraction has a higher tendency to undergo transformation to sp²-carbon structures, confirming a reduced stability toward oxygen exposure and high temperatures.^{98,116,117} Different terminations that can be provided by the amorphous carbon network can produce cumulene or polyyne structures, respectively.⁸⁸ Short cumulenes can be synthesized in a similar way by playing with termination-induced electronic arrangement. Such strategy has been discussed in the review by Cadierno et al.,¹¹⁸ and the synthesis of cumulene wires was reported by Cataldo¹¹⁹ and more recently by Tykwinski and co-workers^{82,83} which described cumulenes wires up to 8 sp-carbon atoms produced by means of stepwise chemical synthesis. In all of these systems, the choice terminal groups for the cumulene is fundamental for multiple reasons. For example, aromatic endgroups can strongly couple with the sp-chain, which then propagates through the wire structure. On the other hand, bulky endgroups are necessary in order to prevent intermolecular interactions among wires, and thus avoiding cross-linking reactions and conversion into amorphous sp²-carbon, as discussed also for polyynes.

4. Raman, IR and SERS spectroscopy of carbon wires: recent investigations

4.1 Raman and SERS spectroscopy of carbon wires

As mentioned above, the vibrational structure of CAW depends on the length of the wire. This is important when dealing with the Raman active modes associated to C-C stretching vibrations. DFT calculations of the Raman response of differently endcapped CAWs clearly show the marked dispersion of the strong Raman active mode associated to the BLA oscillation as a function of the number of sp-carbon atoms in the chain.^{75,86,120} This sp-chain length dependence can be observed in Fig. 14 for the case of phenyl-endcapped polyynes. The wavenumber of the characteristic Raman modes (BLA oscillation) sensibly decreases for increasing sp-chain length. DFT calculations⁸⁶ and experiments⁸⁹ also show that the Raman intensity of these BLA-oscillation modes (ECC mode) promptly increases with chain length, and it is sensitive to the coupling with π -conjugated caps, as it has been recently reported for cumulene-like systems.¹²⁰ Although the correct Raman intensity behaviour as a function of chain length is not described very accurately by DFT methods, by summing up the contributions from each chain length (weighted by their abundance in the sample), however, one can obtain a reasonable representation of the experimental spectra in hydrogen-endcapped polyynes⁸⁶ and phenyl-endcapped polyynes.⁷⁹ This approach allows the interpretation of the main Raman features of the spectra of CAWs samples containing a distribution of chain lengths. Amongst the wires investigated in detail by Raman spectroscopy we mention polyynes terminated with hydrogen, metal atoms, phenyl and naphthalene groups, as well as systems with bulkier endgroups such as those synthesized by Tykwinski and coworkers.

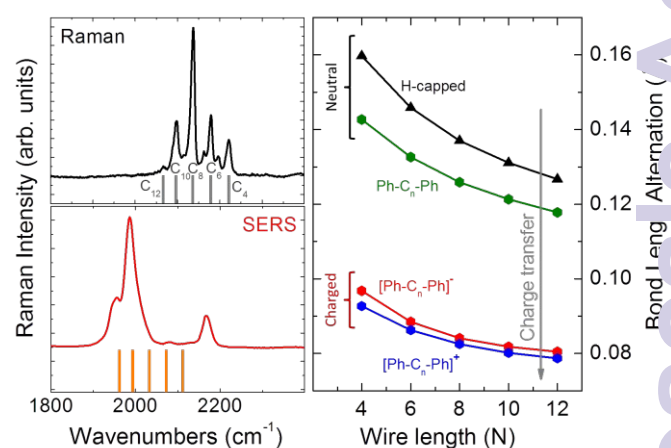


Figure 14: Left panels: Experimental Raman and SERS spectra (1064 nm) of phenyl-endcapped polyynes on silver nanoparticles, as the SERS-active medium. Lines show theoretical position of peaks as a function of wire length according to DFT calculation of the Raman modes (PBE0/cc-pVTZ).⁷⁹ Right panel: BLA values as a function of wire length for neutral and charged phenyl endcapped (Ph-endcapped) polyynes. BLA values of neutral H-endcapped polyynes are also shown for comparison.

Hydrogen termination results in limited stability over time and the wire show transition towards sp^2 -carbon structures as a consequence of cross-linking reactions.¹¹² Bulkier endgroups provide higher stability to CAWs. As an example, phenyl-endcapped polyynes (Ph- C_n -Ph) up to $n = 12$ are stable at ambient conditions even in a solid film when the solvent is completely removed.⁷⁹ The Raman spectrum of samples of phenyl-endcapped polyynes with a distribution of chain lengths is characterized by well-resolved peaks in the 2050–2250 cm^{-1} region. As depicted in Fig. 14, these features can be traced back to the distribution of sp -chain lengths in the sample. DFT calculations of the Raman spectra of phenyl-endcapped polyynes of selected lengths show a significant red shift of the ECC mode for increasing chain lengths, consistently with the increase of π -conjugation.

SERS is commonly employed to increase the sensitivity of Raman spectroscopy by many orders of magnitude sometimes reaching the single molecule level. It is based on the local enhancement of the electromagnetic field due to a resonance with surface plasmons present in metal nanoparticles. In addition to this enhancement (i.e., electromagnetic SERS effect) there is also the possibility that the investigated system forms a complex with the metal nanoparticles due to charge transfer resulting in an additional enhancement that is usually called chemical SERS effect. In the case of hydrogen endcapped polyynes, we observed an enhancement factor of 10^6 with respect to normal Raman response.⁸⁶ A peculiar effect is observed when hydrogen- and phenyl-endcapped polyynes interact with noble metal nanoparticles (i.e., silver and gold), such as those considered for SERS to increase the sensitivity of the Raman technique.⁷⁹ We observe that the SERS spectrum is quite different from the Raman spectrum. A red-shift of the main Raman feature is accompanied by the appearance of new spectral features at lower wavenumbers (i.e., below 2000 cm^{-1}), as shown in Fig. 14 for the case of diphenyl polyynes on silver nanoparticles. Similar spectral changes (i.e., from Raman to SERS) are also observed in the case of gold nanoparticles for different excitation wavelengths ranging from NIR to blue (1064–458 nm), suggesting that it is not a resonance-activated effect.⁷⁹

4.2 Charge transfer effects in CAWs

The spectral changes occurring upon interaction with metal nanoparticles, which are observed when comparing Raman with SERS (see above), suggest a chemical SERS effect with total enhancement factors up to 10^6 (observed for hydrogen-endcapped polyynes).⁸⁶ A charge transfer between the metal and the carbon wire has been invoked to explain these remarkable spectral changes.⁷⁹ In fact, by comparing ECC Raman frequencies calculated on neutral and charged CAWs a relevant softening of the Raman modes and an increase of the intensity is observed for charged wires, as reported in Fig. 14. For instance, for a CAW of $n = 8$ carbon atoms, a decrease of about 100 cm^{-1} upon charging the wire is predicted, both by adding or removing one electron. These theoretical predictions indicate that, upon charge transfer, new Raman peaks would appear in the spectra at lower wavenumbers and with a higher Raman intensity, than found for neutral wires. By evaluating the energy required for the formation of the two possible

charged configurations one can determine the direction of the charge transfer. The configuration with a positively charged metal and negatively charged wire turns out to be energetically favoured. Since charge transfer alters the electronic properties of the wire, effects on the structure are also expected, due to the characteristic and strong electron-phonon coupling that exists in π -conjugated systems.⁷¹ Charge transfer induces a decrease of BLA in the sp -carbon chain (Fig. 14), indicating that the wire evolves from alternated (polyynelike) to more equalized (cumulene-like) wire configuration upon charge transfer. The reduction amounts to more than 30% for a singly charged wire and more than 60% for a doubly charged wire, reaching a lower value of 0.04 Å for 12 carbon atoms. Recently synthesized cumulenes⁸² show an experimental BLA value as low as 0.038 Å at the central bond in the longest cumulene (formed by 9 C=C bonds). This compares well with the asymptotic BLA value of anionic phenyl-endcapped polyynes (Fig. 14) that can be thus considered to essentially possess a cumulene-like structure. Finally, it is important to remark that for finite-length wires the ideal cumulene structure with BLA = 0 Å is not realistic due to the influence of the endgroups. The endgroup effects are stronger in shorter wires (see Fig. 9, where the BLA of finite cumulene-like systems is reported).

4.3 Vibrational spectroscopy of excited states

Another case demonstrating the existence of cumulene-like species can be found in ref. 117 where IR spectroscopy has been used to explain sp -carbon wires with cumulene-like geometry induced by external effects, in particular the occurrence of photo-generated species trapped in a forbidden electronic state. In Fig. 15, IR spectra after photo excitation are reported. After photo irradiation at low temperature, a new band at about 2130 cm^{-1} appears in the IR spectrum, suggesting the photo generation of a new molecular species with particular vibrational and, hence, structural properties. Furthermore, by increasing the temperature, this band disappears, demonstrating that the process is reversible and should not be ascribed to any kind of degradation or transformation of the system. DFT calculations revealed that this feature can be ascribed to molecule trapped in either the S_1 or T_1 excited state and which possesses a strong cumulene-like character with a very small value of BLA.¹¹⁷ These results demonstrate the possibility of observing and detecting cumulene-like CAWs and are among the first where the occurrence of these systems have been indeed established by means of experimental measurements. These experiments demonstrate the coupling between electronic and vibrational properties and verify the importance of investigating the excitation dynamics of sp -carbon wires, which are characterized by subtle and delicate phenomena involving different excited states. This latter point has been recently demonstrated by means of state-of-the-art experimental techniques.¹²¹

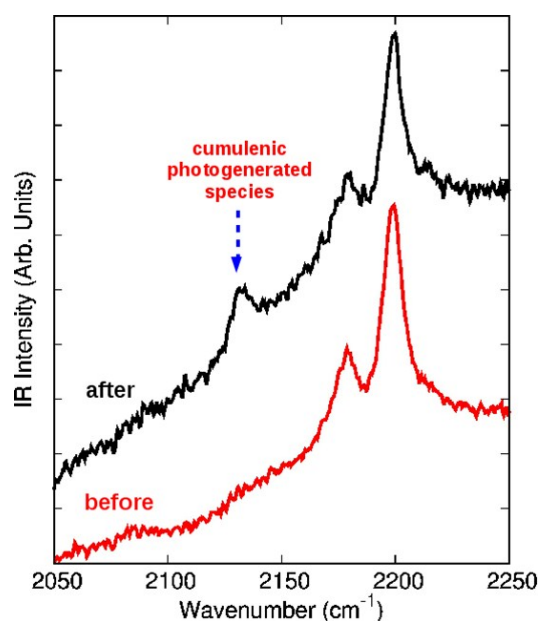


Figure 15: IR spectra of adamantyl endcapped C_{12} polyynes embedded in a PMMA matrix: before and after UV irradiation with a 325 nm line recorded at 78 K. The evolution of a new feature (associated to photo generated cumulene-like species) is evident. Adapted with permission from ref. 117, copyright 2011 AIP Publishing LLC.

4.4 The peculiar Raman response of cumulene-like systems

Long cumulenes have been recently synthesized in the Tykwinski group,⁸² thus offering opportunity to compare molecular characteristics to the other sp -carbon wires. The cumulene-like systems are composed of 3, 5, 7 and 9 cumulated $C=C$ bonds, and they are endcapped with aryl moieties (see Fig. 16). X-ray diffraction studies reveal that the BLA of these aryl endcapped cumulenes is substantially lower than that of a polyynes of comparable chain length, which is also substantiated by DFT calculations.¹²⁰ However, the structural data as a function of wire length reveal a trend which appears to reach a limit before a cumulene-like structure with $BLA = 0$ is achieved.⁸² This could indicate the onset of Peierls distortion, similarly to what has been reported by Kertesz on uncapped sp -carbon wires.⁸⁴ Since the endgroups contribute to π -conjugation, however, a definitive explanation would require specific theoretical investigations, which are still lacking. Raman spectroscopy¹²⁰ of these long cumulenes has shown the direct implication of aryl groups to π -conjugation along the sp -chain through the unusually strong ECC Raman features, which are typical of bond-alternated (semiconductive) structures. Still, the observed low frequency of the ECC Raman signals indicates a system characterized by a low BLA (see Fig. 17). Compared with polyynes of similar chain length and termination,⁷⁶ cumulenes display a significantly less selective Raman signal, characterized by CC stretching lines attributed to the sp -chain (ECC) and to endgroups (Fig. 17). At a first glance, this different behaviour may be due to a decrease of the Raman intensity of ECC modes in cumulenes compared to the endgroup modes, in contrast to the behaviour of polyynes for which ECC modes are strong and dominate over endgroup modes.⁸⁹

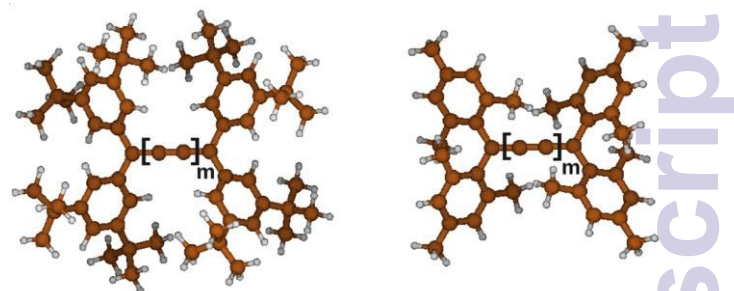


Figure 16 Molecular structures of cumulenes: **tBuPh**[n] (left) and **Mes**[n] (right); $n = m + 2$ indicates the number of cumulated double bonds in the carbon chain.

However, a closer comparison of experimental data normalized with respect to the weak CH stretching signals (Fig. 17) reveals that the ECC signal of cumulene **tBuPh**[7] is comparable to that of a polyynes with similar chain length, **SP**[4] and the phenyl modes of the cumulene are significantly stronger than those of the polyynes, which are barely observed as shown in Fig. 17.

DFT calculations reveal that the frontier orbitals of cumulenes, as expected, are delocalized over the sp -chain, but also significantly involve the aryl moieties of the endgroups. This behaviour is not observed in adamantyl endcapped polyynes, **Ad**[n] for which, in fact, we do not observe strong Raman modes of endgroups compared to the modes of the wire. The interesting interplay of aryl groups with the cumulene chain may offer opportunities for the fine-tuning of the molecular properties of cumulenes by proper chemical functionalization.

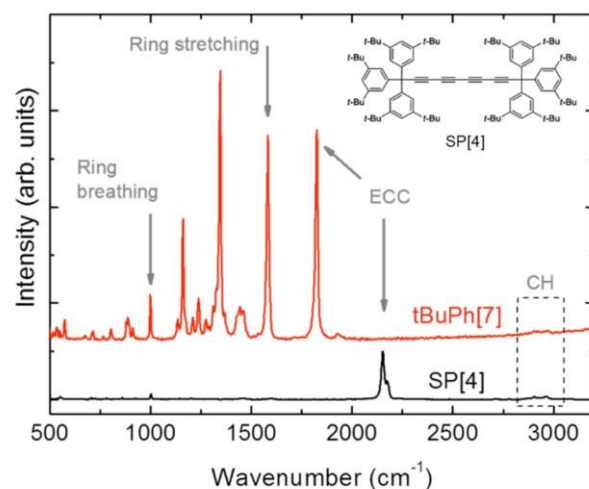


Figure 17 Experimental FT-Raman spectra of polyynes **SP**[4] (black) and cumulene **[7]tBuPh**, (red) normalized with respect to the aliphatic CH-stretching region. The structure of polyynes **SP**[N] is shown in the inset, the structure of **tBuPh**[M] is shown in Fig. 16. Adapted with permission from ref. 120, copyright 2014, American Chemical Society.

5. Potential applications, novel structures and future perspectives

As described in the previous sections, the structural tunability of CAWs implies that mechanical, electronic, and optical properties can be modulated to a wide extent, thus making these systems quite appealing for applications. Some efforts aimed at investigating the characteristics of sp-carbon systems have adopted advanced pump-probe techniques¹²¹ in order to characterize the dynamical evolution of electronic states and electrical measurements to assess the transport properties. The unusual behaviour of CAWs still deserves a complete rationalization and will surely represent a fertile ground for future investigations.

5.1 Optical and mechanical properties

CAWs should be ideal systems to investigate the nonlinear optical (NLO) properties of 1-D conjugated systems. This hypothesis was first explored by two different methods. First, the non-resonant molecular second hyperpolarizabilities (γ_{ele}) for the CAWs endcapped with silyl groups (**TIPS[n]**) were determined using the differential optical Kerr effect (DOKE),¹²² and γ -values show a power law increase as a function of length (n) (Fig. 18).^{123,124} This power law behaviour was stronger than theoretically predicted for polyynes, and it was higher than that reported for polyenes and polyynes. The second method evaluated the NLO behaviour based on the vibrational contribution to the second hyperpolarizability (γ_{vib}) for adamantyl endcapped CAWs (**Ad[n]**), using the quantitative Raman spectra and the Raman scattering intensities that correspond to the polyyne.^{125,126} It was quite remarkable that the γ_{vib} values showed very similar behaviour with respect to chain length.⁸⁹ It has been shown that the nature of the endgroups is negligible for longer CAWs in the two series based on UV/vis spectroscopy,¹²⁷ and it was thus reasonable to conclude that the origin of the NLO behaviour in both cases derived primarily from the sp-hybridized carbon chain.¹²⁸

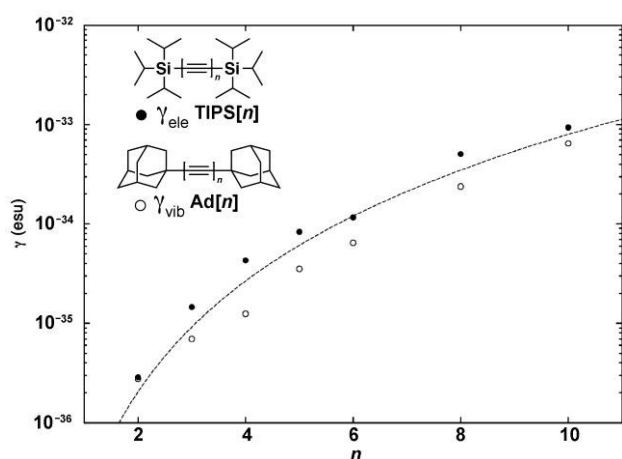


Figure 18 Experimental γ_{ele} (●) and electronic γ_{vib} (○) values for **TIPS[n]** and **Ad[n]** polyynes, respectively, as a function of chain length (semi-log scale). The dashed line is a power-law fit to both datasets and it is meant only as a guide to the eye.

The combined linear and nonlinear optical results from these studies implied that polyynes might function as ideal

conjugated systems,¹²⁹ which has motivated other studies of the NLO behaviour of sp-carbon containing systems,^{130,131} including optical limiting applications.¹³²

According to their structure and bond coordination CAWs can be expected to show very good mechanical properties. sp² Hybridization should ensure an extremely high tensile strength that may outperform nanotubes and graphene. In recent years some papers have focused on theoretical calculations of mechanical properties of these systems, as 1-D wires with extraordinary properties.¹³³⁻¹³⁶

5.2 Transport properties

The interest in CAWs as conducting or functional wires comes from a wealth of theoretical studies pointing out the unique electronic and conductance properties of isolated systems. Pioneering theoretical investigations by Lang and Avouris showed an oscillatory behaviour with the number of carbon atoms of the conductance properties of wires contacted by gold leads.^{9,10} In particular even-numbered wires are predicted to display lower conductance than odd-numbered wires. This is related to the density of states (DOS) behaviour at the Fermi level that is higher for even-numbered wires due to different population of the HOMO level and the mixing with metal states of the electrodes. Odd-numbered CAWs show constant conductance behaviour with wire length. Conductivity values are close to the theoretical maximum of $2G_0$, where $G_0 = 2e^2/h = 77 \mu\text{S}$ (equivalent to a resistance of 12.9 k Ω) is the quantum of conductance, according to Landauer formula.¹³⁷ For even-numbered wires the conductance increases with the number of carbon atoms indicating that the perturbation of the metal leads is more pronounced in short systems. The relevant charge transfer from the metal to the chain is considered to play an effective role in the conductance as a sort of doping effect that add electrons to the partially filled HOMO level in even-numbered wires, while it contributes to the LUMO of odd-numbered wires that have a completely filled HOMO level.^{9,138}

Larade et al. have predicted a transport regime characterized by negative differential resistance for CAWs connected to Al electrodes.¹³⁸ The effect of strain and doping on the transport properties of infinite cumulene wires has been addressed by Tongay et al.¹¹ Considering an electrode-wire-electrode configuration where metallic CAWs are used as electrodes, unstrained wires show quantum-ballistic transport with a constant conductance of $2G_0$ for electron energy in a wide range around Fermi level, while the application of a strain produces the appearance of an oscillatory behaviour of conductance values as a function of electron energy. Yakobson and coworkers have investigated the bandgap dependence of mechanical strain pointing out a strain induced metal-to-insulator transition. On one hand, they show that in a free unstrained chain the zero-point vibrational energy overcome the barrier for the Peierls transition allowing the existence of a long cumulene chain with metallic character. On the other hand, they underline that strain can be used to modify such effect to favour polyyne form with insulating behaviour.^{77,139}

While polyyne-like wires are expected to display metallic-like conductance when chemisorbed on metals like gold,¹³⁰ recently, graphene sheets or nanoribbons have been also considered as contact electrodes.^{141,142} In particular graphene-wire-graphene systems are appealing as a pure carbon-based model for nanoscale-devices in which the linear energy dependence of the conductance in graphene can lead to a unique behaviour. Zanolli et al.¹⁴² showed that wires connected with graphene edges with zigzag or armchair structure show magnetic properties and spin-dependent transport. In general the magnetization is strongly related to the chain structure. No magnetization is observed in even-numbered wires while odd-numbered wires show a net magnetization due to the local presence of uncompensated charge. In any case, the occurrence of spin polarization appears to be an intrinsic property of the wire that does not depend on the magnetization of the contacts.

Only a few studies have reported on the experimental transport properties of CAWs. The reason can be mainly due to the difficulty to have CAWs with controlled properties. The conductivity of disordered sp^2 -carbon systems has been measured *in situ* as a function of the polyyne and cumulene content showing the contribution of sp -carbon to the electrical conductivity of the whole system.⁹⁸ Moving to single molecule transport Wang et al. firstly reported a measurement of the conduction of single CAWs by means of the STM-break junction method.¹⁴³ Such method is based on using the STM metal tip and a metal substrate as the two contacts of a molecular junction. By changing the tip-to-substrate distance, molecular junctions are repeatedly formed and broken. A plateau in the current-distance curve (at a given bias) indicates the molecular conductance. The same measurements can be performed by applying a mechanical strain that can induce formation of a wire bridging two fragments (i.e., the so called mechanical-break junction method). A comparative study with both the techniques was conducted by Moreno-García et al. on wires with different lengths.^{144,145} The measured conductivity is much lower than the one predicted by ballistic conductance and this has been explained by the complex interaction between the terminations and the contact leads. Pt-encapped polyynes have been explored experimentally in single molecule junctions. This work shows that vibronic features can be detected as satellites to the electronic transitions, which are assigned to longitudinal modes of the wires by theoretical studies.¹⁴⁶

By shrinking a carbon nanotube under a TEM to induce narrowing, Yuzvinsky et al. measured conductance as a function of the tube diameter. Just before breaking, they observed a negative differential resistance, but no information on the nature of the connecting carbon chain was given.¹⁴⁷ In this context, the detailed and systematic investigation of the conducting properties of CAW-based systems is an almost unexplored field. A few representative examples are reported in Fig. 19.

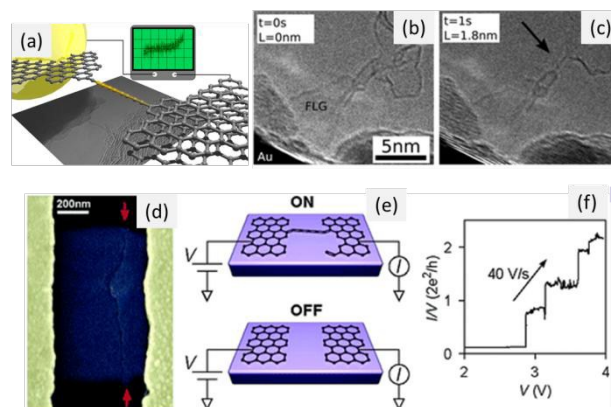


Figure 19 Transport properties measurement of single CAWs: (a–c) Production by TEM technique and *in situ* measurement of wires suspended between graphene flakes (reprinted with permission from ref. 150, copyright 2013, American Chemical Society); (d–f) graphene-based memristor device based on mechanically-induced formation and breaking of wires (Reprinted with permission from ref. 146, copyright 2013, American Chemical Society).

A memory device based on forming and breaking wires by mechanical stress of graphene has been reported.¹⁴⁸ Recently, F. Banhart and co-workers reported the measurements of transport properties in single CAWs suspended between graphene edges.^{7,149,150} The system was fabricated in a TEM, starting from graphene and *in situ* characterized. In particular by measuring wires under strain they were able to observe a change in current-voltage curves indicating a metal-semiconductor transition.¹⁵⁰ Such experimental results are in agreement with theoretical predictions, as discussed before.

5.3 CAWs integrated with sp^2 -carbon

Some possible systems where CAWs are integrated with sp^2 -carbon nanostructures are depicted in Fig. 20. The formation of an atomic junction between carbon nanotubes has been observed at the end of a shrinking procedure made by mechanical pulling.¹⁵¹ CAWs have been observed in the core of carbon nanotubes (both single and multiple-wall), as evidenced by TEM pictures of carbon nanotubes with regions showing apparently an odd number of walls one of which lay on the tube axis.²⁹ Carbon nanotubes act as a protecting cage for CAWs thus permitting the observation of long wires probably up to hundreds of carbon atoms. Hydrogen-encapped CAWs produced by laser ablation in liquids are able to fill the inner core of both multi- and single-wall carbon nanotubes. The tube protection allows processing the system at high temperature to promote formation of long wires.¹⁵² Graphene has been considered as a natural termination for CAWs, either to have a pure carbon system with stable endgroups or as carbon-based electrodes for ideal device set up. Graphene can induce well-defined wire organization depending on the type of bonding site provided for CAW anchoring, i.e., sp^2 -sites are likely to promote cumulene-type while sp^3 -sites will induce polyyne-like organization. This can be used for the interpretation of the Raman spectrum of sp - sp^2 -amorphous carbon moieties where additional torsional and bending effects must be taken into account.⁸⁸

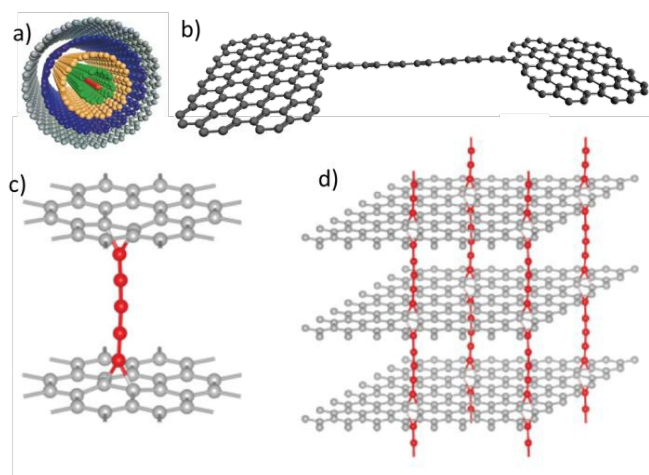


Figure 20 Examples of carbon atomic wires integrated in sp^2 -carbon nanostructures: a) CAW in the core of a carbon nanotube; b) CAW suspended between two graphene edges; c) CAW vertically grown from a graphene flake and d) sp - sp^2 -architecture comprising stacked graphene planes kept separated by CAWs. (Panel a) is reprinted with permission from ref. 29, copyright 2003 by American Physical Society. Panels c) and d) are reprinted with permission from ref. 155, copyright 2011 by American Physical Society.)

A system built from two graphene edges connected by a CAW has been investigated by numerical simulations for unveiling transport properties, as discussed above. Such an architecture is not only intriguing for theoretical predictions, but it has been recently realized and imaged by a TEM-based approach.^{7,31,110,111} CAWs between graphene domains have been realized but, even with TEM images showing the atomic structure of the chain, no evidence of either cumulene or polyene structure was given.¹¹¹ New insight into the structure of CAWs has been recently provided indicating a possible bond alternation in wires suspended between graphene edges.³¹ The possibility to produce CAWs by pulling a graphene flake was theoretically investigated showing that the formation of polyene-like wires at the graphene edge are favoured by the presence of dimers and topological defects.^{153,154} The perpendicular growth of CAWs connecting graphene sheets has been theoretically considered, toward producing carbon atomic pillars on graphene layers and even stacked layers kept separated by wires of selected lengths (see Fig. 20).¹⁵⁵ A bottom-up route to CAWs connected to graphene is represented by wires endcapped by coronene molecules as shown by numerical simulations.¹⁵⁶ The computational investigation of CAWs bonded to moieties containing conjugated sp^2 -carbon atoms was carried out in the case of phenyl- and naphthyl-endcapped polyynes,^{79,157,158} demonstrating that these systems should show new chemical/physical phenomena deserving investigation. The occurrence and structure of CAWs as local defects of disordered carbon clusters were studied by simulating the rapid quenching of carbon vapours.¹⁰⁰ On the other hand, the coagulation of CAWs in sp - sp^2 -networks has been observed as well.^{23,159}

5.4 sp - sp^2 -hybrid architectures: graphynes and related novel structures

A number of intriguing structures can be conceived by combining sp - and sp^2 -carbon atoms, including 2-D crystals, such as graphynes and graphdiynes (see e.g., the review by Ivanovskii).¹⁶⁰ Such structures have been first outlined in 1981 by Baughman, Eckhardt and Kertesz.¹⁶¹ One simple example is given by using linear $-C\equiv C-$ bonds to connect sp^2 -carbon hexagons thus producing the so-called γ -graphyne or 6,6,6-graphyne (see Fig. 21). Another possibility is to construct a honeycomb structure made by linear bonds only (both cumulene-like and polyene-like), as a sp -carbon counterpart of graphene, called α -graphyne or 18,18,18-graphyne. The nomenclature is based on three numbers indicating the number of carbon atoms in the smallest ring, in the next ring that is connected to the first one by a linear $-C\equiv C-$ bond, and in the ring that is in *ortho*-position with respect to the previous two rings, respectively. According to this, α -graphyne is 18,18,18-graphyne while γ -graphyne is 6,6,6-graphyne. The carbon content can vary from 75% in α -graphyne, to 66.67% in 12,12,12-graphyne (β -graphyne), 55% for 6,6,12-graphyne, and down to 50% for 6,6,6-graphyne.

Similar systems, graphdiynes, can be obtained by replacing a single acetylenic linkage with a double one (i.e., $-C\equiv C-C=C-$). The 6,6,6-graphdiyne structure has been reported by Haley et al.¹⁶² as the most stable structure with diacetylenic units. According to theoretical predictions such systems should show appealing electronic, optical, and mechanical properties. The presence of linear bonds should result in an increase of the Poisson's ratio and decrease of in-plane stiffness with respect to graphene, while the bending stiffness is comparable. As in the case of single wires, graphyne shows a tunable gap when the system is under strain. The electronic properties have been computed for different structures showing the presence of Dirac's cones in K and K' points for 18,18,18-graphyne, as occurs in graphene. 12,12,12-Graphyne shows Dirac's cones in a low symmetry point along the ΓM direction, as outlined by Goerling and co-workers.¹⁶³

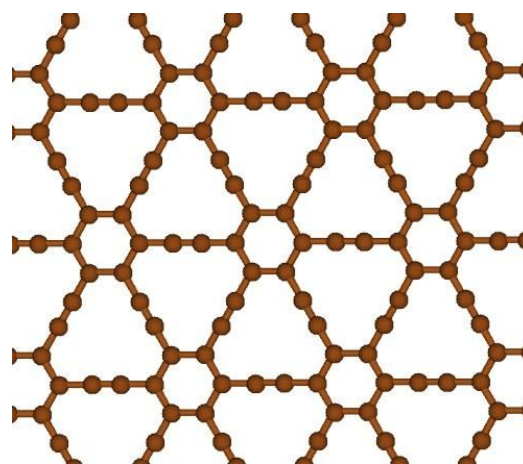


Figure 21 Structure of γ -graphyne (6,6,6-graphyne)

They have also shown that Dirac's cones can occur in 2-D systems in the presence of hetero-atoms (e.g., $6_{\text{BN}}, 6_{12}$ and $6(\text{H}_2)$, 14,18-graphyne derivatives) and even with rectangular structure, as the 6,6,12-graphyne, pointing out that hexagonal symmetry (as in the case of both 18,18,18- and 12,12,12-graphyne) is not required for the existence of Dirac points (see Fig. 22).^{163,164} As a result of such a peculiar electronic properties, high charge carrier mobility has been predicted for these systems, comparable to graphene ($\mu = 3 \times 10^5 \text{ cm}^2 \text{ V}^{-1} \text{ s}^{-1}$). 6,6,12-Graphyne should show a mobility value for both electron and holes at least along one direction that could outperform graphene (i.e., about $5 \times 10^5 \text{ cm}^2 \text{ V}^{-1} \text{ s}^{-1}$ for electrons). The vibrational properties have been calculated by Popov and Lambin for α -, β -, and γ -graphynes to focus on Raman active modes and on the predicted Raman spectrum.¹⁶⁵ Zone centre phonons below 1000 cm^{-1} are related to bending modes, stretching modes appear at about 1000 cm^{-1} while stretching vibrations involving single and triple bonds are expected in the $2000\text{--}2200 \text{ cm}^{-1}$ spectral region as in CAWs. All the Raman-active modes are in-plane. For example, in α -graphyne the G-mode-like phonon is reduced to about 1000 cm^{-1} with a softening of about 50% with respect to the G mode in graphene or graphite (1582 cm^{-1}). Starting from graphyne and graphdiyne as hybrid sp-sp^2 -counterparts of graphene, a number of novel structures can be considered such as graphyne nanoribbons, nanotubes and fullerene-like cage structures (see e.g., review of ref. 160). For nanoribbons the energy gap increases with decreasing the ribbon width while nanotubes are expected to show metallic/semiconducting behaviour depending on the chirality as for conventional sp^2 -carbon nanotubes.¹⁶⁶⁻¹⁶⁸ Theoretical results indicate a great potential for such systems, however, experimental works dealing with synthesis, characterization and application are still lacking.

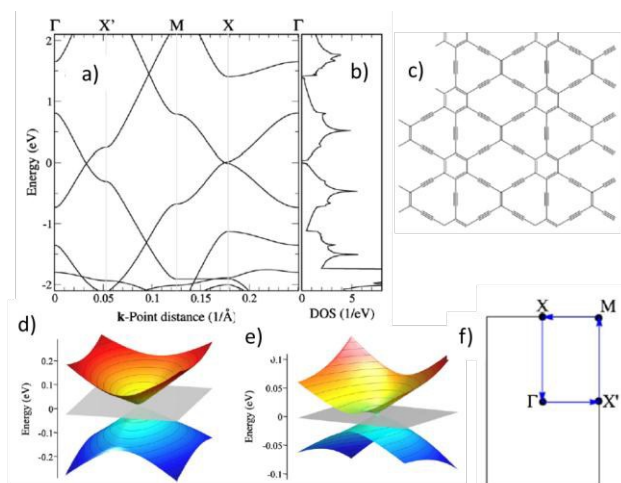


Figure 22 a) Electronic structure and b) density of states of 6,6,12-graphyne. The structure in the direct space is represented in c). The two different Dirac's cones appearing along the ΓM directions are represented in d) and e). The unit cell in the reciprocal space is schematized in f). Reprinted with permission from ref. 163, copyright 2012 by American Physical Society.

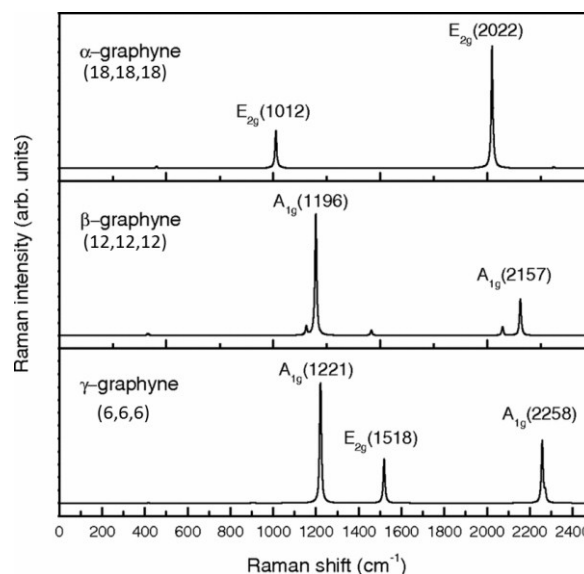


Figure 23 Simulated Raman spectra of different types of graphyne systems. Reprinted with permission from ref. 165, copyright 2013 by American Physical Society

A work reported the synthesis of extended graphdiyne films even though there is no direct evidence of the ordered structure of the system.¹⁶⁵ On the contrary, sp-sp^2 -carbon molecular building blocks for extended graphyne and graphdienes have been produced by Diederich and co-workers,^{170,171} by Haley and co-workers^{162,172-174} and by other groups.¹⁷⁵

Very recently conductivity measurements have been performed on model sp-sp^2 -molecules (i.e., carbo-benzene and carbo-n-butadiene) at the single molecule level by means of the scanning tunnelling microscopy break junction method.¹⁷⁶ Such systems can be considered as fundamental building blocks of extended α -graphyne systems even though they have been endcapped with suitable anchoring groups to be connected with metal electrodes (i.e., the tip and the substrate). In the case of carbo-benzene results show single molecule conductance of about 100 nS that is very high with respect to similar molecular fragments. As an example such reported value is larger than a molecular fragment mimicking graphene (i.e., hexabenzocoronene) showing, with the same technique, a conductance of 14 nS on a shorter distance (1.4 nm instead of 1.94 nm). The reason for this performance is to be ascribed to the macro-aromatic ring that provides a rigid planar conformation, as supported by the comparison with other molecular fragments with a different degree of conformational rigidity.¹⁷⁶

A network of wires decorated by calcium atoms has been proposed as efficient material for H storage, as a result of numerical calculations.¹⁷⁷ Possible architectures comprise wire-graphene system and a 3-D network of wires joined by sp^3 links to form a diamond-like lattice.

While it is clear that theory predicts great potential for sp-sp^2 hybrids in nanotechnology applications, experimental results are obviously still needed. A few recent experiments confi-

the peculiar properties of such systems at least at the level of molecular fragments, thus underlining that there is still a lot of work to fill the large gap between theory and experiments.

6. Conclusions and outlook

In this review we have discussed sp-carbon nanostructures to underline the striking properties expected and, in some cases, observed in these systems. Carbon-atom wires are true 1-D systems with strong structure-property relationships that allow tuning of optical and electronic behaviour of these materials over a broad range of desired applications. Even though the existence of carbyne as the 'third carbon allotrope' is still controversial, sp-carbon nanostructures and molecules can now often be synthesized in stable forms and subsequently investigated. The structure and, hence, functional properties of CAWs can be designed by playing with wire length (i.e., number of carbon atoms) and endgroups. This opens the possibility to provide a new library of nanoscale systems with properties ranging from metallic through semiconducting to insulating. Such systems are appealing for many aspects of carbon science and have a great potential in fields such as nano/molecular electronics and optoelectronics, as functional molecules, nanoscale structures and as assembled systems and molecular materials, just to name a few. In addition, the great interest in the properties of graphene has driven the attention to hybrid sp-sp² architectures such as graphynes and graphdiynes. These 2-D materials and their molecular counterparts could show properties that might even be superior to graphene (e.g., charge carrier mobility, variable bandgap, multiple Dirac's cones, and behaviour as a topological insulator) as outlined by theoretical predictions. In this framework, there is also an obvious synergy between CAWs and graphene technologies, through the integration of sp-carbon segments with graphene structures, such as wires bridging graphene edges or suspended between graphene planes. The seemingly limitless potential of sp-carbon-based nanoscale systems has been suggested in many theoretical works, while we have only scraped the surface of discoveries in the experimental realm. There is, thus, a lot of work still to be done in order to unveil the potential of this "new" player in the vast family of carbon-based materials.

Acknowledgements

Funding in Erlangen from the Deutsche Forschungsgemeinschaft (DFG - SFB 953, "Synthetic Carbon Allotropes") is gratefully acknowledged.

References

- 1 A. Hirsch, *Nat. Mater.*, 2010, **9**, 868.
- 2 M. Dresselhaus, G. Dresselhaus, P.C. Eklund, *Science of Fullerenes and Carbon Nanotubes*, Academic Press 1995
- 3 A. H. Castro Neto, F. Guinea, N. M. R. Peres, K. S. Novoselov, and A. K. Geim *Rev. Mod. Phys.* 2009, **81**, 109
- 4 M. I. Knatsnelson *Graphene, Carbon in Two Dimensions*, Cambridge Univ. Press, 2013
- 5 A.C. Ferrari, F. Bonaccorso, V. Fal'ko et al., *Nanoscale* 2015, **7**, 4598-4810
- 6 H.-S. Philip Wong and Deji Akinwande, *Carbon Nanotube and Graphene Device Physics*, Editore: Cambridge University Press, 2011
- 7 F. Banhart *Beilstein J. Nanotechnol.*, 2015, **6**, 559-569
- 8 A. Milani, M. Tommasini, V. Russo, A. Li Bassi, A. Lucotti, F. Cataldo, C.S. Casari *Beilstein J. Nanotechnol.*, 2015, **6**, 480-491.
- 9 N. D. Lang and Ph. Avouris, *Phys. Rev. Lett.*, 2000, **85**, 358.
- 10 N.Lang, P.Avouris, *Phys. Rev. Lett.* 1998, **81**, 3515-3518.
- 11 S. Tongay, R. T. Senger, S. Dag, and S. Ciraci, *Phys. Rev. Lett.*, 2004, **93**, 136404.
- 12 S. Tennant, *Philosophical Transactions of the Royal Society of London*, 1797, **87**, 123-127.
- 13 R. B. Heimann, S. E. Evsyukov, L. Kavan, *Carbyne and Carbynyoid Structures*, Kluwer Academic Publishers, 1999.
- 14 A. El Goresy and G. Donnay, *Science*, 1968, **161**, 363.
- 15 A. G. Whittaker and P. L. Kintner, *Science*, 1969, **165**, 589.
- 16 A.G. Whittaker, *Science*, 1978, **200**, 763.
- 17 P. P. K. Smith and P. R. Buseck, *Science*, 1982, **216**, 984.
- 18 A. G. Whittaker, *Science*, 1985, **229**, 485.
- 19 P. P. K. Smith and P. R. Buseck, *Science*, 1985, **229**, 486.
- 20 H. Kroto, *Rev. Mod. Phys.*, 1997, **69**, 703.
- 21 R. H. Baughman, *Science* 312, 1009 2006.
- 22 F. Cataldo, *Polyynes: Synthesis, Properties, and Applications*, Taylor & Francis, 2005
- 23 T. Wakabayashi, A. L. Ong, D. Strelnikov and W. Krätschmer, *J. Phys. Chem. B*, 2004, **108**, 3686.
- 24 L. Ravagnan, F. Siviero, C.S. Casari, A. Li Bassi, C. Lenardi, C.E. Bottani, P. Milani, *Carbon* 2005, **43**, 1337-1339
- 25 L. Ravagnan, T. Mazza, G. Bongiorno, M. Devetta, M. Amati, P. Milani, P. Piseri, M. Coreno, C. Lenardi, F. Evangelista and P. Rudolf, *Chem. Commun.*, 2011, **4**, 2952.
- 26 A. A. Zaidi, A. Hu, M. J. Wesolowski, X. Fu, J. H. Sanderson, Y. Zhou, W. W. Duley, *Carbon*, 2010, **48**, 2517.
- 27 L. Ravagnan, F. Siviero, C. Lenardi, P. Piseri, E. Barborini, P. Milani, C. S. Casari, A. Li Bassi and C. E. Bottani, *Phys. Rev. Lett.*, 2002, **89**, 285506.
- 28 H. Tabata, M. Fujii and S. Hayashi, *Carbon*, 2006, **44**, 522.
- 29 X. Zhao, Y. Ando, Y. Liu, M. Jinno, and T. Suzuki, *Phys. Rev. Lett.*, 2003, **90**, 187401.
- 30 C. Jin, H. Lan, L. Peng, K. Suenaga and S. Iijima, *Phys. Rev. Lett.*, 2009, **102**, 205501.
- 31 G. Casillas, A. Mayoral, M. Liu, A. Ponce, V. I. Artyukhov, B.I. Yakobson, M. Jose-Yacamán *Carbon*, 2014, **66**, 430-441
- 32 Y. Wang, Y. Huang, B. Yang and R Liu, *Carbon*, 2006, **44**, 456.
- 33 E. Cazzanelli, M. Castriota, L. S. Caputi, A. Cupolillo, C. Giallombardo and L. Papagno, *Phys. Rev. B*, 2007, **75**, 121405R.
- 34 D. Nishide, H. Dohi, T. Wakabayashi, E. Nishibori, S. Aoyagi, M. Ishida, S. Kikuchi, R. Kitaura, T. Sugai, M. Sakata and H. Shinohara, *Chem. Phys. Lett.*, 2006, **428**, 356.

- 35 D. Nishide, T. Wakabayashi, T. Sugai, R. Kitaura, H. Kataura, Y. Achiba and H. Shinohara, *J. Phys. Chem. C*, 2007, **111**, 5178.
- 36 W.A. Chalifoux, Rik R. Tykwinski *Nature Chemistry* 2010, **2**, 967–971
- 37 A. Mendoza, Y. Ishihara, P.S. Baran *Nature Chemistry* 2012, **4**, 21–25
- 38 R. O. Jones and G. Seifert, *Phys. Rev. Lett.*, 1997, **79**, 443.
- 39 M. Saito and Y. Okamoto, *Phys. Rev. B*, 1999, **60**, 8939.
- 40 T. Torelli and L. Mitas, *Phys. Rev. Lett.*, 2000, **85**, 1702.
- 41 A. Abdurahman, A. Shukla, and M. Dolg, *Phys. Rev. B*, 2002, **65**, 115106.
- 42 A. Karpfen, *J. Phys. C*, 1979, **12**, 3227.
- 43 M. Springborg, *J. Phys. C*, 1986, **19**, 4473.
- 44 A. Ruzsnyak, V. Zolyomi, J. Kurti, S. Yang and M. Kertesz, *Phys. Rev. B*, 2005, **72**, 155420.
- 45 U. Molder, P. Burk and I. A. Koppel, *J. Mol. Struct.*, 2004, **712**, 81.
- 46 M. Kertesz and S. Yang, *Phys. Chem. Chem. Phys.*, 2009, **11**, 425.
- 47 Y. Liu, R. O. Jones, X. Zhao and Y. Ando, *Phys. Rev. B*, 2003, **68**, 125413.
- 48 R. Zbinden, *Infrared Spectroscopy of High Polymers*, Academic Press, 1964.
- 49 P. C. Painter, M. M. Coleman and J. L. Koenig, *The Theory of Vibrational Spectroscopy and Its Application to Polymeric Materials*, Wiley & Sons, 1982.
- 50 G. Zerbi, in *Advances in Infrared and Raman spectroscopy*, vol. 11, R. J. H. Clark, R. R. Hester Eds, Wiley 1984, 301.
- 51 C. Castiglioni, in *Vibrational Spectroscopy of Polymers: Principles and Practices*, N. J. Everall, J.M. Chalmers, P. R. Griffiths Eds, Wiley, 2007, 455.
- 52 M. Del Zoppo, C. Castiglioni, P. Zuliani, G. Zerbi, in *Handbook of Conductive Polymers 2nd Ed.*, T. Skotheim, R. L. Elsembaumer, J. Reynolds Eds, Dekker, 1998, 765.
- 53 R. Hoffmann, *Tetrahedron* 1966, **22**, 521-538
- 54 A. Milani, M. Tommasini, M. Del Zoppo, C. Castiglioni, and G. Zerbi, *Phys. Rev. B*, 2006, **74**, 153418.
- 55 A. Milani, M. Tommasini, G. Zerbi, *J. Chem. Phys.* 2008, **128**, 064501.
- 56 W. A. Chalifoux, R. McDonald, Michael J. Ferguson, Rik R. Tykwinski, *Angew. Chem. Int. Ed.*, 2009, **48**, 7915–7919.
- 57 R. E. Peierls, *Quantum Theory of Solids*, Oxford University Press, 2001.
- 58 R. Hoffmann, *Angew. Chem. Int. Ed.*, 1987, **26**, 846–878.
- 59 A. Milani, M. Tommasini, D. Fazzi, C. Castiglioni, M. Del Zoppo, and G. Zerbi, *J. Raman Spectrosc.*, 2008, **39**, 164.
- 60 N. W. Ashcroft, N. D. Mermin, *Solid State Physics*, Saunders, 1976.
- 61 F. Innocenti, A. Milani and C. Castiglioni, *J. Raman Spectrosc.*, 2010, **41**, 226.
- 62 M. Tommasini, A. Milani, D. Fazzi, M. Del Zoppo, C. Castiglioni, and G. Zerbi, *Physica E*, 2008, **40**, 2570.
- 63 S. Pisanec, M. Lazzeri, F. Mauri, A.C. Ferrari and J. Robertson, *Phys. Rev. Lett.*, 2004, **93**, 185503.
- 64 M. Lazzeri, S. Pisanec, F. Mauri, A.C. Ferrari and J. Robertson, *Phys. Rev. B*, 2006, **73**, 155426.
- 65 S. Pisanec, M. Lazzeri, J. Robertson, A.C. Ferrari and F. Mauri, *Phys. Rev. B*, 2006, **75**, 035427.
- 66 E. Di Donato, M. Tommasini, C. Castiglioni and G. Zerbi, *Phys. Rev. B*, 2006, **74**, 184306.
- 67 G. Zerbi, in *Vibrational Spectroscopy of Polymers: Principles and Practice*, N. J. Everall, J. M. Chalmers, P. R. Griffiths Eds, Wiley, 2007, 487.
- 68 C. Castiglioni, M. Gussoni, J. T. Lopez-Navarrete and G. Zerbi, *Solid State Commun.*, 1988, **65**, 625.
- 69 C. Castiglioni, M. Tommasini and G. Zerbi, *Phil. Trans. R. Soc. Lond. A*, 2004, **362**, 2425.
- 70 E. Ehrenfreund, Z. Vardeny, O. Brafman and B. Horowitz, *Phys. Rev. B*, 1987, **36**, 1535.
- 71 A. Milani, M. Tommasini and G. Zerbi, *J. Raman Spectrosc.*, 2009, **40**, 1931.
- 72 E. B. Wilson, J. C. Decius, and P. C. Cross, *Molecular Vibrations: The Theory of Infrared and Raman Vibrational Spectra*, Dover, 1980.
- 73 M. Tommasini, D. Fazzi, A. Milani, M. Del Zoppo, C. Castiglioni and G. Zerbi, *J. Phys. Chem. A*, 2007, **111**, 11645.
- 74 C. Mapelli, C. Castiglioni, G. Zerbi, and K. Müllen, *Phys. Rev. B*, 1999, **60**, 12710.
- 75 A. Lucotti, M. Tommasini, D. Fazzi, M. Del Zoppo, W. A. Chalifoux, M. J. Ferguson, G. Zerbi, and R. R. Tykwinski, *J. Am. Chem. Soc.*, 2009, **131**, 4239.
- 76 N. R. Agarwal, A. Lucotti, D. Fazzi, M. Tommasini, C. Castiglioni, W. A. Chalifoux and R. R. Tykwinski, *J. Raman Spectrosc.* 2013, **44**, 1398.
- 77 Vasilii I. Artyukhov, Mingjie Liu, and Boris I. Yakobson, *Nano Lett.*, **2014**, *14* (8), pp 4224–4229
- 78 M. Kertesz, C. Ho Choi, S. Yang *Chem. Rev.* 2005, **105**, 3448
- 79 A. Milani, A. Lucotti, V. Russo, M. Tommasini, F. Cataldo, A. Li Bassi, C. S. Casari, *J. Phys. Chem. C*, 2011, **115**, 12836.
- 80 S. Yang, M. Kertesz, V. Zolyomi and J. Kurti, *J. Phys. Chem. A*, 2007, **111**, 2434.
- 81 S. Yang and M. Kertesz, *J. Phys. Chem. A*, 2008, **112**, 146
- 82 J. A. Januszewski, D. Wendinger, C. D. Methfessel, J. Hampel and R. R. Tykwinski, *Angew. Chem., Int. Ed.* 2013, **52**, 1817.
- 83 J. A. Januszewski and R. R. Tykwinski, *Chem. Soc. Rev.*, 2014, **43**, 3184.
- 84 S. Yang and M. Kertesz, *J. Phys. Chem. A*, 2006, **110**, 9771.
- 85 M. Tommasini, D. Fazzi, A. Milani, M. Del Zoppo, C. Castiglioni, and G. Zerbi, *Chem. Phys. Lett.*, 2007, **450**, 86.
- 86 A. Lucotti, M. Tommasini, M. Del Zoppo, C. Castiglioni, G. Zerbi, F. Cataldo, C. S. Casari, A. Li Bassi, V. Russo, M. Bogana, and C. E. Bottani, *Chem. Phys. Lett.*, 2006, **427**, 78.
- 87 H. Tabata, M. Fujii, S. Hayashi, T. Doi, and T. Wakabayashi, *Carbon*, 2006, **44**, 3168.
- 88 L. Ravagnan, N. Manini, E. Cinquanta, G. Onida, L. Sangalli, C. Motta, M. Devetta, A. Bordoni, P. Piseri and P. Milani, *Phys. Rev. Lett.*, 2009, **102**, 245502.
- 89 A. Lucotti, M. Tommasini, D. Fazzi, M. Del Zoppo, W. A. Chalifoux, R. R. Tykwinski and G. Zerbi, *J. Raman Spectrosc.*, 2012, **43**, 1293.
- 90 C. S. Casari, A. Li Bassi, L. Ravagnan, F. Siviero, C. Lenardi, P. Piseri, G. Bongiorno, C. E. Bottani, and P. Milani, *Phys. Rev. B*, 2004, **69**, 075422.
- 91 D. A. Long, *The Raman Effect: A Unified Treatment of the Theory of Raman Scattering by Molecules*, John Wiley & Sons, 2002.
- 92 M. Jevric, M.B. Nielsen, *Asian J. Org. Chem.* 2015, **4**, 286
- 93 S. Szafert and J. A. Gladysz, *Chem. Rev.*, 2003, **103**, 4171
- 94 P. Milani, S. Iannotta, *Cluster Beam Synthesis of Nanostructured Materials* Springer 1999
- 95 G. Compagnini, S. Battiato, O. Puglisi, G. A. Baratta, and G. Strazzulla, *Carbon*, 2005, **43**, 3025
- 96 T. Wakabayashi, H. Nagayama, K. Daigoku, Y. Kiyooka, K. Hashimoto *Chemical Physics Letters* 2007, **446**, 65–70

- 97 A Hu et al. *J Chem Phys* 2007, **126**, 154705
- 98 L. Ravagnan, P. Piseri, M. Bruzzi, S. Miglio, G. Bongiorno, A. Baserga, C. S. Casari, A. Li Bassi, C. Lenardi, Y. Yamaguchi, T. Wakabayashi, C. E. Bottani and P. Milani, *Phys. Rev. Lett.*, 2007, **98**, 216103.
- 99 L. Ravagnan, G. Bongiorno, D. Bandiera, E. Salis, P. Piseri, P. Milani, C. Lenardi, M. Coreno, M. de Simone, and K. C. Prince, *Carbon*, 2006, **44**, 1518
- 100 M. Bogana, L. Ravagnan, C. S. Casari, A. Zivelonghi, A. Baserga, A. Li Bassi, C. E. Bottani, S. Vinati, E. Salis, P. Piseri, E. Barborini, L. Colombo and P. Milani, *New J. Phys.*, 2005, **7**, 81.
- 101 H. Tabata, M. Fujii, and S. Hayashi, *Chem. Phys. Lett.*, 2006, **420**, 166.
- 102 A. Hu, M. Rybachuk, Q.-B. Lu and W. W. Duley, *App. Phys. Lett.*, 2007, **91**, 131906.
- 103 F. Cataldo, *Carbon*, 2003, **41**, 2671.
- 104 F. Cataldo, *Tetrahedron*, 2004, **60**, 4265.
- 105 Y.P. Kudryavtsev, R.B. Heimann, S.E. Evsyukov, *J. Mater. Sci.* 1996, **31**, 5557.
- 106 Y. P. Kudryavtsev, S.E. Evsyukov, M.B. Guseva, V.G. Babaev, V.V. Khvostov, *Russian Chemical Bulletin* 1993, **42**, 399.
- 107 P. Siemsen, R.C. Livingston, F. Diederich, *Angew. Chem. Int. Ed.* 2000, **39**, 2633.
- 108 W. A. Chalifoux, R.R. Tykwinski, *C.R. Chim.* 2009, **12**, 341.
- 109 R. Tykwinski, *Chem. Rec.* 2015 doi: 10.1002/tcr.201500018.
- 110 E. Kano, M. Takeguchi, J. Fujita, A. Hashimoto *Carbon*, 2014, **80**, 382-386.
- 111 C. Jin, H. Lan, L. Peng, K. Suenaga and S. Iijima, *Phys. Rev. Lett.*, 2009, **102**, 205501.
- 112 A. Lucotti, C. S. Casari, M. Tommasini, A. Li Bassi, D. Fazzi, V. Russo, M. Del Zoppo, C. Castiglioni, F. Cataldo, C. E. Bottani and G. Zerbi, *Chem. Phys. Lett.*, 2009, **478**, 45.
- 113 C. S. Casari, V. Russo, A. Li Bassi, C. E. Bottani, F. Cataldo, A. Lucotti, M. Tommasini, M. Del Zoppo, C. Castiglioni, and G. Zerbi, *Appl. Phys. Lett.*, 2007, **90**, 013111.
- 114 S. Okada, M. Fujii and S. Hayashi, *Carbon*, 2011, **49**, 4704.
- 115 F. Cataldo and C. S. Casari, *J. Inorg. Organomet. Polym. Mater.*, 2007, **17**, 641.
- 116 C. S. Casari, A. Li Bassi, A. Baserga, L. Ravagnan, P. Piseri, C. Lenardi, M. Tommasini, A. Milani, D. Fazzi, C. E. Bottani and P. Milani, *Phys. Rev. B*, 2008, **77**, 195444.
- 117 M. M. Yildizhan, D. Fazzi, A. Milani, L. Brambilla, M. Del Zoppo, W. Chalifoux, R. R. Tykwinski and G. Zerbi, *J. Chem. Phys.*, 2011, **134**, 124512
- 118 V. Cadierno and J. Gimeno, *Chem. Rev.*, 2009, **109**, 3512.
- 119 F. Cataldo, *J. Inorg. Organomet. Polym. Mater.*, 2006, **16**, 15.
- 120 M. Tommasini, A. Milani, D. Fazzi, A. Lucotti, C. Castiglioni, J.A. Januszewski, D. Wendinger, R.R. Tykwinski, *J. Phys. Chem. C* 2014, **118**, 26415–26425
- 121 D. Fazzi, F. Scotognella, A. Milani, D. Brida, C. Manzoni, E. Cinquanta, M. Devetta, L. Ravagnan, P. Milani, F. Cataldo, L. Lueer, R. Wannemacher, J. Cabanillas-Gonzalez, M. Negro, S. Stagira and C. Vozzi, *Phys. Chem. Chem. Phys.*, 2013, **15**, 9384.
- 122 A. D. Slepko, F. A. Hegmann, Y. Zhao, R. R. Tykwinski, K. Kamada, *J. Chem. Phys.* **2002**, **116**, 3834–3840.
- 123 S. Eisler, A. D. Slepko, E. Elliott, T. Luu, R. McDonald, F. A. Hegmann, R. R. Tykwinski, *J. Am. Chem. Soc.* **2005**, **127**, 2666–2676
- 124 A. D. Slepko, F. A. Hegmann, S. Eisler, E. Elliott, R. R. Tykwinski, *J. Chem. Phys.* 2004, **120**, 6807–6810.
- 125 C. Castiglioni, M. Del Zoppo, P. Zuliani, G. Zerbi, *Synth. Met.* 1995, **74**, 171–177.
- 126 M. Rumi, G. Zerbi, K. Müllen, G. Müller, M. Rehahn, *J. Chem. Phys.* 1997, **106**, 24–34.
- 127 R. R. Tykwinski, W. Chalifoux, S. Eisler, A. Lucotti, M. Tommasini, D. Fazzi, M. Del Zoppo, G. Zerbi, *Pure Appl. Chem.* 2010, **82**, 891–904.
- 128 C. Castiglioni, M. Del Zoppo, G. Zerbi, *Phys. Rev. B* 1996, **53**, 13319–13325.
- 129 M. G. Kuzyk, *Phys. Rev. Lett.* 2000, **85**, 1218–1221; erratum: *ibid.*, 2003, **90**, 039902.
- 130 T. Luu, E. Elliott, A. D. Slepko, S. Eisler, R. McDonald, F. A. Hegmann, R. R. Tykwinski, *Org. Lett.* 2005, **7**, 51–54.
- 131 J. C. May, J. H. Lim, I. Biaggio, N. N. P. Moonen, T. Michinobu, F. Diederich, *Opt. Lett.* 2005, **30**, 3057–3059
- 132 E. Fazio, S. Patanè, L. D'Urso, G. Compagnini and F. Neri, *Opt. Comm.* 2012, **285**, 2942.
- 133 A. Arendt, R. Kolkowski, M. Samoc, S. Szafert, *Phys. Chem. Chem. Phys.* 2015, **17**, 13680–13688.
- 134 G.-L. Xu, C.-Y. Wang, Y.-H. Ni, T. G. Goodson III, T. Ren, *Organometallics*, 2005, **24**, 3247–3254.
- 135 E. Fazio, L. D'Urso, G. Consiglio, A. Giuffrida, G. Compagnini, O. Puglisi, S. Patane, F. Neri, G. Forte, *Phys. Chem. C* 2014, **118**, 28812–28819.
- 136 M. Samoc, G. T. Dalton, J. A. Gladysz, Q. Zheng, V. Velkov, H. Agren, P. Norman and M. G. Humphrey, *Inorg. Chem.* 2008, **47**, 9946–9957.
- 137 R. Landauer, *IBM Journal of Research and Development*, 1957, **1**, 223–231.
- 138 B. Larade, J. Taylor, H. Mehrez, H. Guo *Phys. Rev. B* 2001, **64**, 075420
- 139 M. Liu, V.I. Artyukhov, H. Lee, F. Xu, B.I. Yakobson *ACS Nano*, 2013, **7** (11), 10075–10082
- 140 Z. Crljen, G. Baranovic, *Phys Rev Lett* 2007, **98**, 116801
- 141 W. Chen et al. *Phys Rev B* 2009, **80**, 085410
- 142 Z. Zanolli, G. Onida, J.C. Charlier, *ACS Nano* 2010, **4**, 5174.
- 143 C. Wang, A.S. Batsanov, M.R. Bryce, S. Martín, R.J. Nichols, S.J. Higgins, V.M. García-Suarez, C.J. Lambert, *Am. Chem. Soc.* 2009, **131**, 15647–15654.
- 144 P. Moreno-García, M. Gulcur, D. Zsolt Manrique, T. Pope, W. Hong, V. Kaliginedi, C. Huang, A. S. Batsanov, M.R. Bryce, C. Lambert, T. Wandlowski *J. Am. Chem. Soc.* 2013, **135**, 12228–12240
- 145 M. Gulcur, P. Moreno-García, X. Zhao, M. Baghernejad, A. S. Batsanov, W. Hong, M.R. Bryce, T. Wandlowski, *Chem. Eur. J.*, 2014, **20**, 4653–4660.
- 146 S. Ballmann, W. Hieringer, D. Secker, Q. Zheng, J. A. Gladysz, A. Görling, H.B. Weber, *Chem Phys Chem*, 2011, **11**, 2256–2260.
- 147 T.D. Yuzvinsky et al. *Nano Lett* 2006, **6**, 2718
- 148 B. Standley, W. Bao, H. Zhang, J. Bruck, C. Ning Lau and M. Bockrath, *Nano Lett.*, 2008, **8** (10), 3345–3349
- 149 O. Cretu et al. *Nano Lett.*, **2013**, **13** (8), pp 3487–3493
- 150 A. La Torre, A. Botello-Mendez, W. Baaziz, J. -C. Charlie, F. Banhart *Nature Communications* 2015, **6**, 6636
- 151 H.E. Troiani, M. Miki-Yoshida, G. A. Camacho-Bragado, M. A. L. Marques, A. Rubio, J. A. Ascencio, M. Jose-Yacamán *Nano Lett.* 2003, **3**, 751
- 152 C. Zhao et al., *J. Phys. Chem. C* 2011 **115**, 13166
- 153 E. Hobi et al. *Phys Rev B* 2010, **81**, 201406
- 154 Y. Wang et al. *Phys Rev B* 2007, **76**, 165423
- 155 C. Ataca et al. *Phys Rev B* 2011, **83**, 235417
- 156 R. Rivelino et al. *J Phys Chem C* 2010, **114**, 16367
- 157 E. Cinquanta et al. *J Chem Phys* 2011, **135**, 194501
- 158 F. Cataldo et al. *J Phys Chem* 2010, **B 114**, 14834
- 159 Y. Yamaguchi et al. *Chem Phys Lett* 2004, **388**, 436

- 160 A.L. Ivanovskii *Progress in Solid State Chemistry* 2013, **41**, 1
- 161 R.H. Baughman, H. Eckhardt, M. Kertesz *J. Chem Phys* 1987, **87**, 6687
- 162 M.M. Haley *Angew. Chem. Int. Ed.* 1997, **36**, 835
- 163 D. Malko, C. Neiss, F. Viñes, A. Görling *Phys. Rev. Lett.*, 2012, **108**, 086804
- 164 D. Malko, C. Neiss, A. Görling *Phys. Rev. B*, 2012, **86**, 045443
- 165 V.N. Popov, P. Lambin *Phys Rev. B* 2013, **88**, 075427
- 166 H. Bai, Y. Zhu, W. Qiao, Y. Huang *RSC Advances*, 2011, **1**, 768–775
- 167 V.R. Coluci, S.F. Braga, S.B. Legoas, D. S. Galvão, and R. H. Baughman *Phys. Rev. B*, 2003, **68**, 035430
- 168 V.R. Coluci et al *Nanotechnology* 2004, **15**, S142
- 169 G. Li, Y. Li, H. Liu, Y. Guo, Y. Li, D. Zhu. *Chem Commun.* 2010, **46**, 3256–3258
- 170 F. Diederich and M. Kivala, *Adv. Mater.*, 2010, **22**, 803–812.
- 171 P. Rivera-Fuentes and F. Diederich, *Angew. Chem., Int. Ed.*, 2012, **51**, 2818–2828
- 172 M.M. Haley *Pure Appl. Chem.*, 2008, **80**, 519-532
- 173 M. M. Haley, S. C. Brand, J.J. Pak *Angew. Chem. Int. Ed. Engl.* 1997, **36**, 835
- 174 J. M. Kehoe, J.H. Kiley, J. J. English, C. A. Johnson, R. C. Petersen, M. M. Haley, *Organic letters* 2000, **2** 969
- 175 M. Gholami et al. *Chem. Commun.*, 2009, 3038-3040
- 176 Z. Li, M. Smeu, A. Rives, V. Maraval, R. Chauvin, M. A. Ratner, E. Borguet *Nature Communications* 2015, **6**, 6321
- 177 P. B. Sorokin, H. Lee, L. Yu. Antipina, A. K. Singh, B. I. Yakobson *Nano Lett.*, 2011, **11** (7), 2660–2665